

In presenting this thesis as a partial fulfillment of the requirements for an advanced degree from Emory University, I hereby grant to Emory University and its agents the non-exclusive license to archive, make accessible, and display my thesis in whole or in part in all forms of media, now or hereafter known, including display on the world wide web. I understand that I may select some access restrictions as part of the online submission of this thesis. I retain all ownership rights to the copyright of the thesis. I also retain the right to use in future works (such as articles or books) all or part of this thesis.

Signature:

Jason Bothwell

Date

Investigations Into the Design of Electronically Responsive Ligands

By
Jason Bothwell
Master of Science
Chemistry

Christopher C. Scarborough, Ph.D.
Advisor

Lanny S. Liebeskind, Ph.D.
Committee Member

Cora MacBeth, Ph.D.
Committee Member

Accepted:

Lisa A. Tedesco, Ph.D.
Dean of James T. Laney School of Graduate Studies

Date

Investigations Into the Design of Electronically Responsive Ligands

By

Jason Bothwell
B.A., Illinois Wesleyan University, 2010

Advisor: Christopher C. Scarborough, Ph.D.

An abstract of
A thesis submitted to the Faculty of the
James T. Laney School of Graduate Studies of Emory University
in partial fulfillment of the requirements for the degree of
Master of Science
in Chemistry
2013

Abstract

Investigations Into the Design of Electronically Responsive Ligands By Jason Bothwell

The propensity for nickel to undergo sequential one-electron processes has been central in the key elementary steps comprising cross-coupling reactions. Here, we describe our progress in developing a new class of ligands aimed towards facilitating two-electron reactivity at the metal center, reactivity more akin to palladium catalysis. Through intermolecular studies, we show the requisite for stabilizing Ni^0 is a nitroarene or an electron-poor olefin (e.g. maleimide or an α , β -unsaturated carbonyl). Stoichiometric studies have shown nitroarenes lead to the irreversible formation of nickel-black and free ligand, whereas isolable complexes are observed with other ligands. The results of these studies provide the framework for the optimization of future generations of ligands. A comprehensive study on the reactivity of these Ni^0 complexes remains to be explored.

Specific Aims

The first aim of this project is to study the reductive elimination of $(\text{tmeda})\text{Ni}(\text{CH}_3)_2$ in the presence of various π -accepting moieties and gain insight into the structure of the presumed $(\text{tmeda})\text{Ni}^0(\pi\text{-acceptor})$ species. Following this, the design and synthesis of various ligands will begin in order to generate isolable Ni^0 complexes. A study of the reactivity of these Ni^0 complexes may provide insight into the breadth of transformations allowed with the complexes presented herein. If these studies are successful, we aim to provide a new class of catalysts for reactions abiding by the classic $\text{Ni}^0 / \text{Ni}^{\text{II}}$ or $\text{Pd}^0 / \text{Pd}^{\text{II}}$ catalytic cycle, with an emphasis placed on the elucidation of the respective reaction mechanisms.

Investigations Into the Design of Electronically Responsive Ligands

By

Jason Bothwell

B.A., Illinois Wesleyan University, 2010

Advisor: Christopher C. Scarborough, Ph.D.

A Thesis submitted to the Faculty of the
James T. Laney School of Graduate Studies of Emory University
in partial fulfillment of the requirements for the degree of
Master of Science
in Chemistry
2013

Acknowledgements

First and foremost, I would like to thank my P.I., Dr. Chris Scarborough, for accepting me into his lab and allowing me to do research under his supervision. When he arrived at Emory, just a few years ago, I had not realized what my true chemical research interests were. After bonding with Dr. Scarborough in his office discussing chemistry and material from his course, I began critically thinking about what type of research group I would excel in. These thoughts eventually motivated me to switch research groups, prompting Dr. Scarborough to take a pretty big chance on me, seeing that all he knew of me at the time was through my performance in his course. While under his supervision, he provided great feedback on my project and was able to make sure I was not getting lost in the details of research and forgetting the bigger picture of the project.

I would like to thank the members of my committee, Dr. Cora MacBeth and Dr. Lanny Liebeskind, for the thoughts and advice they have provided me. Dr. MacBeth displays an enthusiasm for science that is contagious and is always willing to discuss chemistry with anyone who is willing. She also has been very supportive of my career aspirations, something I am very grateful for. Dr. Liebeskind brings much experience in the field to the table and was able to tell me his thoughts on what it would take for my research to really stand out in the community, a perspective I was excited to hear. He also taught my Organic Spectroscopy course during my first year and his sense of humor made class much more enjoyable, at times when class was not always the most enjoyable. On his final, I received a grade of 100% and when he notified me of this via e-mail he said, "You should try to do better next time."

Along with this, I extend many thanks to my lab mates (Greg Karahalis, Jack Trieu, Arumugam Thangavel, Huaibo Ma, and rotation students Sarah Lauinger and Kevin Sullivan) for making time in lab fun when time in lab was not always the most fun. We stumbled onto many interesting things both inside and outside of lab that I will always remember. I am quite sure I will never forget hearing Greg yell from the other room in lab, only for us to find him dealing with a sodium fire that had made its way onto Greg's jeans. Aru walked up to Greg saying, "You should be careful when working with sodium."

To my family for always being supportive of what I was doing with my life. I always resisted telling them the intricacies of my research, never for a particular reason, but regardless they have been more than supportive of the choices I have made in life. My dad still tells me to this day that I should be working on turning lead into gold. My family has always been enthusiastic with what I am doing and their willingness to help out definitely made things easier at times when things were not that easy. I appreciate that greatly.

People around the facilities of Emory that have definitely led to a more enjoyable experience include Steve and Patty from the stockroom. Every morning I would steal a cup of coffee from them, and Friday's everyone would go to them for free breakfast. A little sugar in the morning goes a long way. Dr. Wu and Bacsa were very pleasant to interact with in the NMR facility and X-ray facility, respectively. Whenever I had a question, they were always available to answer it.

Lastly, to my friends outside of my research group that have made my time at Emory more enjoyable. Naming them is quite difficult but a few do stand out in mind.

Jordan Sumliner has become one of my closest friends here at Emory and has basically been a full time employee of mine, keeping me calm. When we first met, I was unsure how close we would eventually become, but I am quite thankful to have become his friend. A newcomer to Emory, Rebecca Bartlett, has also become very close and inspirational to me during my time here. One of my struggles has been maintaining my focus on the big picture, and not getting trapped in the details – she has helped me with that struggle. I am quite confident she will have a great impact on my life.

Table of Contents

1.	Introduction	1
1.1	Differences Between Nickel and Palladium Catalysis ..	2
1.2	Mechanistic Studies	4
1.3	Oxidatively-Induced Reductive Elimination	8
1.4	Project Inspiration	9
1.5	Electronically Responsive Ligands	10
2.	Results and Discussion	11
2.1	Synthesis and Reactivity of NiL_2X_2 Species	12
2.2	Synthesis of $\text{L}_2\text{Ni}^{\text{II}}(\text{Ph})(\text{Cl})$ Species	14
2.3	Generation of $\text{L}_2\text{Ni}^{\text{II}}(\text{CH}_3)_2$ and Intermolecular Studies ..	16
2.4	Ligand Development	21
3.	Preliminary Metallation Studies	24
4.	Conclusions	25
5.	Experimental Section	27
6.	References	79

List of Schemes

Scheme 1	Pd-catalyzed cross coupling mechanism	1
Scheme 2	Mechanistic analogy of oxidative addition of aryl halides to Pd ⁰	2
Scheme 3	Alkyl-alkyl cross-coupling as reported by Fu	3
Scheme 4	Mechanism of biaryl synthesis reported by Tsou and Kochi.	4
Scheme 5	Nickel-catalyzed cross-coupling as reported by Knochel . .	5
Scheme 6	Cross-coupling mechanism proposed by Knochel	5
Scheme 7	Alkyl-alkyl cross-coupling as reported by Vicic	7
Scheme 8	Alkyl-alkyl cross-coupling as reported by Hu	8
Scheme 9	Reduction of organo(dipyridyl)Ni ^{II} complex as reported by Yamamoto	8
Scheme 10	Reduction of (tmeda)Ni(CH ₃) ₂ as reported by Pörschke . . .	9
Scheme 11	Linkage isomerism of nickel(II) nitrito complexes	10
Scheme 12	Electronically responsive ligand modes of coordination . . .	11
Scheme 13	Divergent route to functionalized diamines	12
Scheme 14	Initially proposed route to stabilized Ni ⁰ complexes	13
Scheme 15	Reactivity of tmeda and teeda with Ni(cod) ₂ and PhCl	15
Scheme 16	Potential reactivity of Ni ^{II} -aryl chloride	15
Scheme 17	Reactions of our diamine ligands with Ni(cod) ₂ and PhCl .	16
Scheme 18	Synthesis of (tmeda)Ni(CH ₃) ₂ as reported by Pörschke	17
Scheme 19	Generation of (tmeda)Ni(acac)AlEt ₂	18
Scheme 20	Generation of (tmeda)Ni(N-Phenylmaleimide)	19
Scheme 21	Synthesis of ligand (1)	22

Scheme 22	Synthesis of ligand (2)	23
Scheme 23	Synthetic strategy towards ligand (3)	23
Scheme 24	Metallation of diamine containing pendant nitroarene	24
Scheme 25	Metallation of diamine containing pendant chalcone	25

List of Tables

Table 1	Calculated LUMO energies of various π -acceptors .	21
---------	--	----

List of Figures

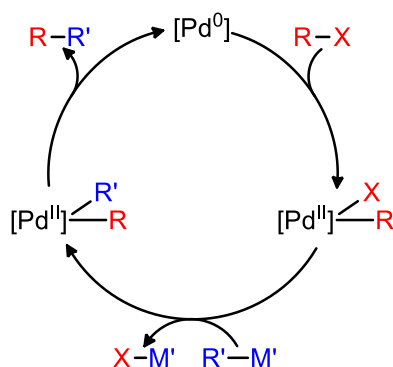
Figure 1	Transmetallation reactions of (1) and (4) with methylmagnesium chloride, as followed by UV-Vis Spectroscopy	14
Figure 2	X-Ray crystal structure of (tmeda)Ni(acac)AlEt ₂ .	18
Figure 3	X-ray structure of (tmeda)Ni(N-Phenylmaleimide)	19
Figure 4	Results of intermolecular study with (tmeda)Ni(CH ₃) ₂ and various π -acceptors	20

List of Abbreviations

°C	degrees Celsius
acac	acetylacetonate
app	apparent
Calcd	calculated
cod	1,5-cyclooctadiene
d	doublet
DMA	N,N'-Dimethylacetamide
DMF	N,N'-Dimethylformamide
en	1,2-ethylenediamine
Equiv	equivalent
EtOAc	ethyl acetate
g	grams
Hex	hexanes
HOMO	Highest Occupied Molecular Orbital
HRMS	High-Resolution Mass Spectrometry
Hz	hertz
J	coupling constant
LUMO	Lowest Unoccupied Molecular Orbital
m	multiplet
Me	methyl
MHz	megahertz
mL	milliliter
mmol	millimoles
NMP	N-Methyl-2-pyrrolidone
Nuc	nucleophile
p	pentet
Ph	phenyl
q	quartet
s	singlet
t	triplet
teda	N,N,N',N'-tetraethylethylenediamine
THF	tetrahydrofuran
tmeda	N,N,N',N'-tetramethylethylenediamine
UV-Vis	ultraviolet-visible
δ	chemical shift (in ppm for NMR)

1. Introduction

In 2010, the Nobel Prize in chemistry was awarded to Professors Heck, Negishi, and Suzuki for their pioneering studies on palladium catalyzed cross coupling.¹ With initial reports focusing on C(sp²) electrophiles, advances amenable to C(sp) electrophiles soon followed.⁵⁻¹¹ The accepted mechanism for palladium catalyzed cross coupling is shown in Scheme 1. C(sp³) electrophiles, on the other hand, presented synthetic challenges that prevented general methods from being established until the mid 1990's,³ despite initial reports being presented in the 1970s.²



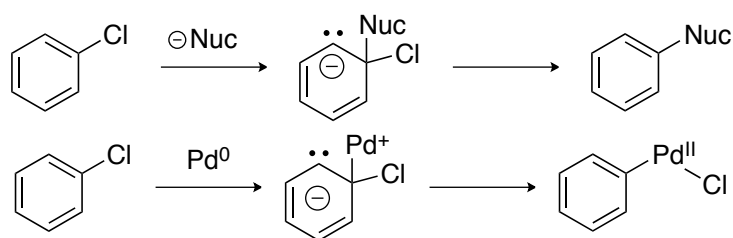
Scheme 1: Pd-catalyzed cross coupling mechanism

While the field of nickel catalysis began earlier, it did not emerge as rapidly as the field of palladium catalysis.⁴ Cross coupling methods tolerant to C(sp³) electrophiles, while difficult with palladium, may be more easily accomplished with nickel due to its lower propensity to undergo β -hydride elimination. Thus, the development of cross coupling methodologies employing nickel catalysis would be highly desired. This is further reinforced when comparing the cost of nickel (\$1.20 / mol) versus the cost of palladium (\$1,500 / mol).⁴

Here, we describe our approach towards the development of ligands designed to facilitate a $\text{Ni}^0 / \text{Ni}^{\text{II}}$ catalytic cycle, reactivity typically observed with palladium-catalyzed cross coupling.

1.1 Differences Between Nickel and Palladium Catalysis

Much is known regarding the requirements of coupling partners utilized in palladium catalyzed cross-coupling methodologies. While studying the oxidative addition of aryl halides to Pd^0 , Stille and Lau related the mechanism to nucleophilic aromatic substitution (Scheme 2).¹²



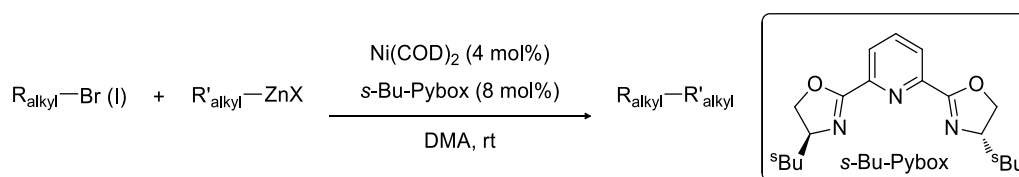
Scheme 2: Mechanistic analogy of oxidative addition of aryl halides to Pd^0

On the other hand, oxidative addition of aryl halides to Ni^0 produces species consistent with a single-electron transfer from the metal center.¹² Kochi also showed the oxidative addition of an aryl halide to $\text{Ni}^0(\text{PEt}_3)_4$ affords both the diamagnetic $\text{Ni}^{\text{II}}(\text{PEt}_3)_2\text{ArX}$ as well as the paramagnetic $\text{Ni}^{\text{I}}(\text{PEt}_3)\text{X}$ in amounts dependent upon both the halide and solvent.¹³

Whereas $\text{C}(\text{sp}^2)$ cross coupling employing palladium catalysis has been widely developed, the use of electrophiles bearing β -hydrogens remains a challenge due to the potential for β -hydride elimination.^{14, 15} β -Hydride elimination of analogous nickel complexes, however, is less prevalent. To explain this observation, Morokuma and co-workers computationally examined the agostic interactions in $\text{M}^{\text{I}}\text{-alkyls}$ ($\text{M} = \text{Ni}, \text{Pd}$), revealing the higher propensity for palladium to undergo β -hydride elimination stems

from a greater interaction between its larger, lower energy d orbitals and the corresponding σ_{CH} orbital, as compared to that of nickel.¹⁶

The lower propensity of nickel to undergo β -hydride elimination may explain the success of nickel in alkyl-alkyl cross coupling, as compared to traditional palladium catalysis. Advances have been made in the area of alkyl-alkyl cross-coupling, with key contributions by Fu and co-workers,¹⁹ who reported that $\text{Ni}(\text{COD})_2$ / (*s*-Bu-Pybox) is an effective catalytic system for the coupling of primary and secondary alkyl bromides with alkylzinc reagents (Scheme 3).



Scheme 3: Alkyl-alkyl cross-coupling as reported by Fu

This represents the first example of a Negishi-like cross-coupling reaction between an unactivated, β -hydride containing, secondary alkyl halide. Fu and co-workers reported the asymmetric variant of this methodology just two years later,²⁰ bringing the synthetic community the first asymmetric cross-coupling of secondary benzylic halides with organozinc reagents.

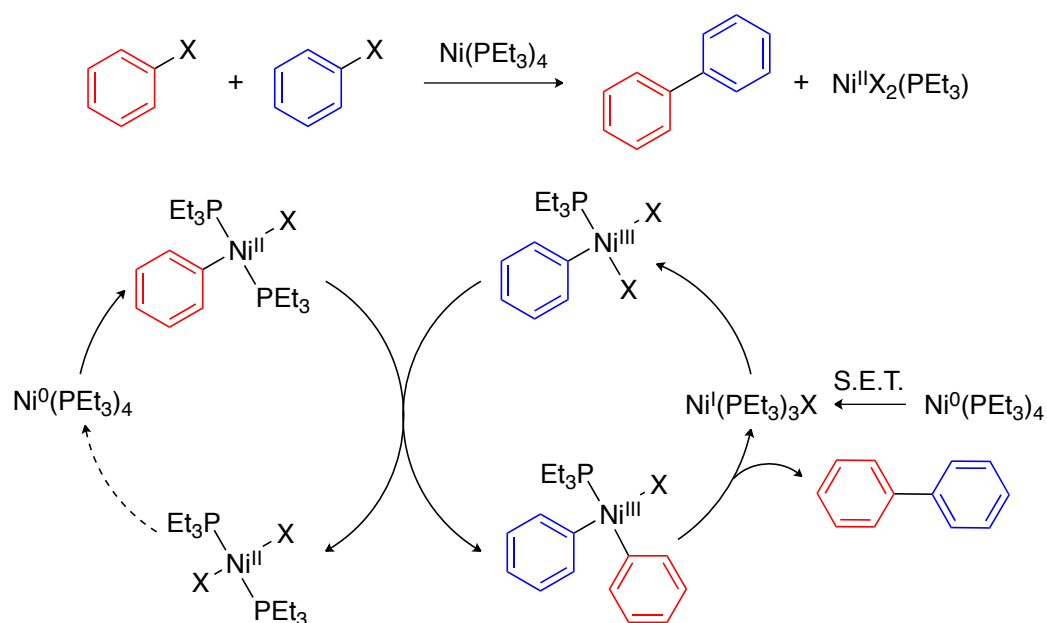
While the nickel catalyzed cross coupling of halogen-containing electrophiles is a well-established area, a significant improvement would be the development of novel methodologies that utilize oxygen-containing electrophiles due to their ubiquity and low cost.⁴ Methodologies accomplishing this have been developed,^{4, 18} however the area has still not come to fruition. For example, one area that has not been widely developed is the cross coupling of alkyl, oxygen-containing electrophiles. One potential complication stems from the ability of nickel to participate in single-electron transfer processes (*vide*

infra). If such a mechanism were invoked with an oxygen-containing electrophile, one would envision the buildup of radical character at oxygen, a thermodynamically disfavored process.³⁰ The development of alkyl-alkyl cross coupling methodologies compatible with oxygen-containing electrophiles would then be highly desirable.

1.2 Mechanistic Studies

While reaction mechanisms featuring palladium are typically understood to proceed according to Scheme 1, pathways involving nickel are not as obvious. Indeed, the ligand has a remarkable effect on the overall reaction mechanism.¹⁵

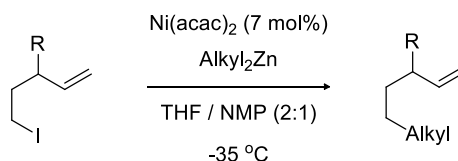
Phosphines, arguably one of the most classic ligand classes, have been widely employed in nickel catalyzed cross coupling for the past few decades. In the late 1970's, Tsou and Kochi reported a detailed mechanistic study on the nickel-phosphine promoted biaryl synthesis, revealing quite an intricate set of elementary pathways. As may be illustrated from the following mechanism (Scheme 4), both $\text{Ni}^0 / \text{Ni}^{\text{II}}$ as well as a $\text{Ni}^{\text{I}} / \text{Ni}^{\text{III}}$ pathways synergistically facilitate the generation of unsymmetric biaryls.³¹



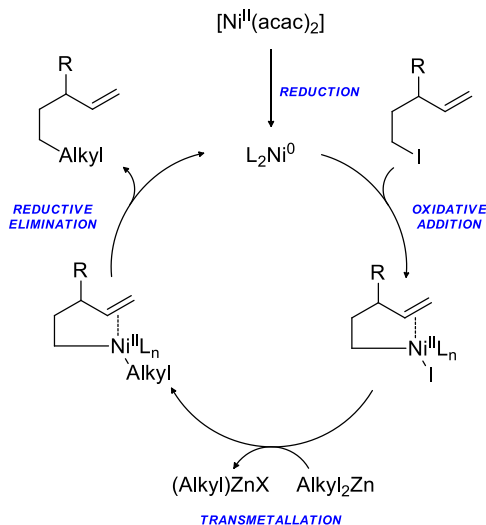
Scheme 4: Mechanism of biaryl synthesis reported by Tsou and Kochi

As the scheme depicts, the overall process is not catalytic with respect to the nickel complex, as the $\text{Ni}(\text{PEt}_3)_2\text{X}_2$ is unreactive. As a result, developments to enable catalysis required stoichiometric reductants.⁴

The first example of a nickel-catalyzed alkyl-alkyl cross coupling was reported in 1995 by Knochel and co-workers, utilizing $[\text{Ni}^{\text{II}}(\text{acac})_2]$ as the catalyst precursor (Scheme 5).³ This reaction was limited to substrates containing a proximal olefin and was shown to accelerate when the olefin was electron deficient. In the absence of a proximal olefin, only transmetalation reaction occurred between the organozinc substrate and the alkyl halide. Scheme 6 shows a proposed mechanism for this transformation.



Scheme 5: Nickel-catalyzed cross-coupling as reported by Knochel

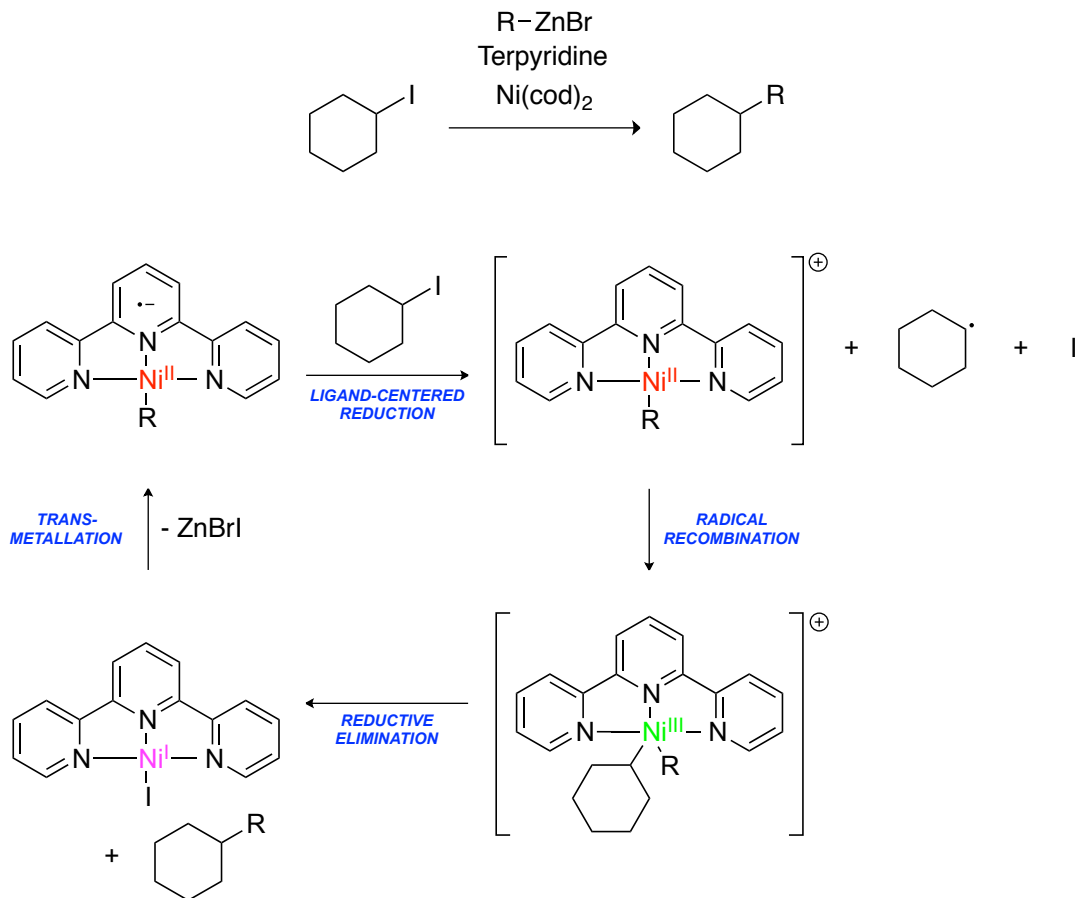


Scheme 6: Cross-coupling mechanism proposed by Knochel

Intuitively, the presence of the proximal olefin facilitated reductive elimination, for in the absence of the olefin the reaction proceeded no further than transmetalation.

Shortly after, Knochel and co-workers reported that in the presence of external additives (e.g. styrene, acetophenone), substrates lacking proximal olefins were able to undergo cross coupling successfully.²¹ Olefins thus represent one class of ligands that facilitate the two-electron reductive elimination of $\text{Ni}^{\text{II}}\text{R}_2$ species.

Moving away from olefins as ligands, Vivic and co-workers have developed alkyl-alkyl cross coupling methodologies employing Ni^{II} (terpyridine) complexes.²² In 2004, they reported the catalytic combination of $\text{Ni}(\text{cod})_2$ and terpyridine facilitates the cross-coupling of alkyl halides and organozinc reagents, with $[\text{Ni}(\text{terpyridine})\text{R}]$ as the proposed, catalytically active species (Scheme 7).^{22a} While the traditional oxidation state formalism suggests the catalytically active species contains a Ni^{I} ion, EPR studies as well as DFT calculations revealed the complex actually contains a central Ni^{II} ion and a one-electron reduced terpyridine ligand.^{22c}

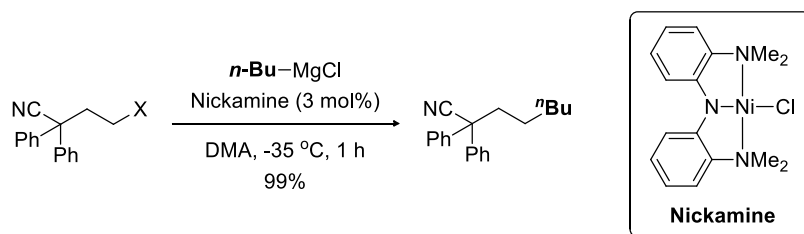


Scheme 7: Alkyl-alkyl cross-coupling as reported by Vicic

The reaction commences with a one electron reduction of the electrophile by $[Ni^{II}(terpyridine)R]$, furnishing an alkyl radical and cationic Ni^{II} complex. A radical addition to the metal generates a five-coordinate Ni^{III} complex, which may then undergo reductive elimination and transmetalation to regenerate the catalytically active species.^{20c} While the mechanistic studies performed by Knochel suggests two-electron reactivity of the metal-center, the system employed by Vicic and co-workers represents a remarkably different mechanism, one comprised of sequential one-electron processes.

Similar to the system reported by Vicic, Hu and co-workers have also explored the area of alkyl-alkyl cross coupling featuring a nickel catalyst (Scheme 8).^{23, 24} Particularly worth merit is the chemoselectivity of the transformation. As may be

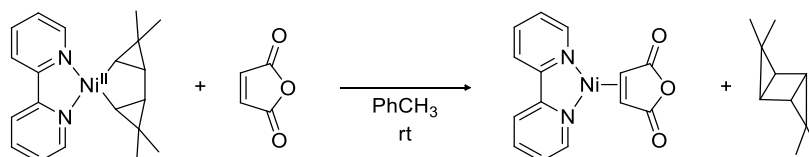
illustrated from Scheme 8, the nitrile moiety is untarnished in the presence of the Grignard reagent. This methodology also has tolerance towards other Grignard-labile moieties, such as esters, amides, and aryl halides. Mechanistic studies suggest similar processes as the Vicic system.^{23, 15}



Scheme 8: Alkyl-alkyl cross-coupling as reported by Hu

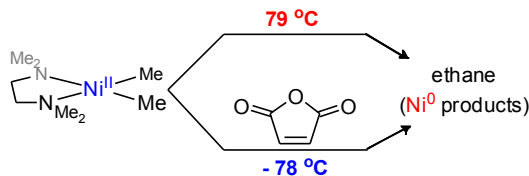
1.3 Oxidatively-Induced Reductive Elimination

In the early 1970's, Yamamoto reported organo(dipyridyl)Ni^{II} complexes, in the presence of various electron-deficient olefins, undergo reductive elimination forging a carbon-carbon bond and an olefin-bound Ni⁰ species (Scheme 9).^{26b}



Scheme 9: Reduction of organo(dipyridyl)Ni^{II} complex as reported by Yamamoto

Pörschke carried out a similar study in 1988 that also highlighted the ability of various electron-deficient olefins to induce reductive elimination of (tmeda)Ni(CH₃)₂ producing an olefin-bound Ni⁰ species (Scheme 10).²⁵ In the absence of the electron-deficient olefin, the Ni^{II}-complex was stable towards decomposition at temperatures nearing 80 °C.



Scheme 10: Reduction of (tmeda)Ni(CH₃)₂ as reported by Pörschke

The ability of the various electron-deficient olefins, in addition to other π -acceptors, to induce reductive elimination was termed ‘oxidatively induced reductive elimination.’^{26b} The effect of the π -acceptor may be visualized in two ways: First, coordination of the metal to the incoming π -acceptor will decrease electron-density at the metal center, favoring reductive elimination. Secondly, as the HOMO of (pseudo)square planar complexes is the metal’s d_z^2 orbital, an addition of the metal to the olefin may be imagined, thereby formally oxidizing the metal center and facilitating reductive elimination.

1.4 Project Inspiration

The overall goal of this research is to enable reactivity of nickel complexes that resembles that of palladium, namely two-electron reactivity featuring Ni⁰ and Ni^{II}. Given the lower propensity of nickel to undergo β -hydride elimination, one goal would be the establishment of alkyl-alkyl cross coupling methodologies featuring oxygen-containing electrophiles. Whereas alkyl-alkyl cross coupling via radical pathways is feasible, there lies a fundamental disconnection as to the lack of progress in oxygen-containing coupling partners. The fact this problem has yet to be comprehensively addressed in the literature may suggest a problem lies in current methods that are comprised of single-electron transfer processes. As a result, targeting Ni⁰ / Ni^{II} catalysis may provide one solution to this problem. If successful, this would stand in contrast to current systems employing

nickel for alkyl-alkyl cross coupling that are comprised of sequential one-electron processes.

1.5 Electronically Responsive Ligands

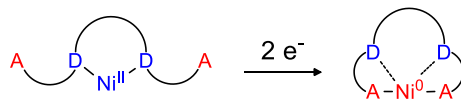
The approach towards the development of ligands that facilitate two-electron transfer from the metal center, specifically Ni^0 , involves the design of ligands that can stabilize both oxidation states successively. These ligands will alter their coordination properties in response to a change in the oxidation state of the metal, favoring low-spin electron configurations. The term these ligands have been given is ‘electronically responsive ligands.’ The broader impact of this research is to introduce to the chemical community a novel ligand class that enables 3d metals to behave like their noble metal counterparts.

The ability of a ligand to vary its mode of coordination as a result of the properties of the metal center has been known for quite some time as linkage isomerism.^{27a} Nickel nitrito complexes represent one classic example of linkage isomerism (Scheme 11).^{27b}



Scheme 11: Linkage isomerism of nickel(II) nitrito complexes

Upon heating, the red dinitro Ni(II) complex is converted into the violet dinitrito Ni(II) isomer. In the context of this project, Ni^0 is well-stabilized by soft, π -accepting ligands, whereas Ni^{II} is stabilized by hard, σ -donating ligands. If a ligand were designed that contained both a π -acceptor as well as a σ -donor, reactivity between Ni^0 and Ni^{II} could be envisioned (Scheme 12).

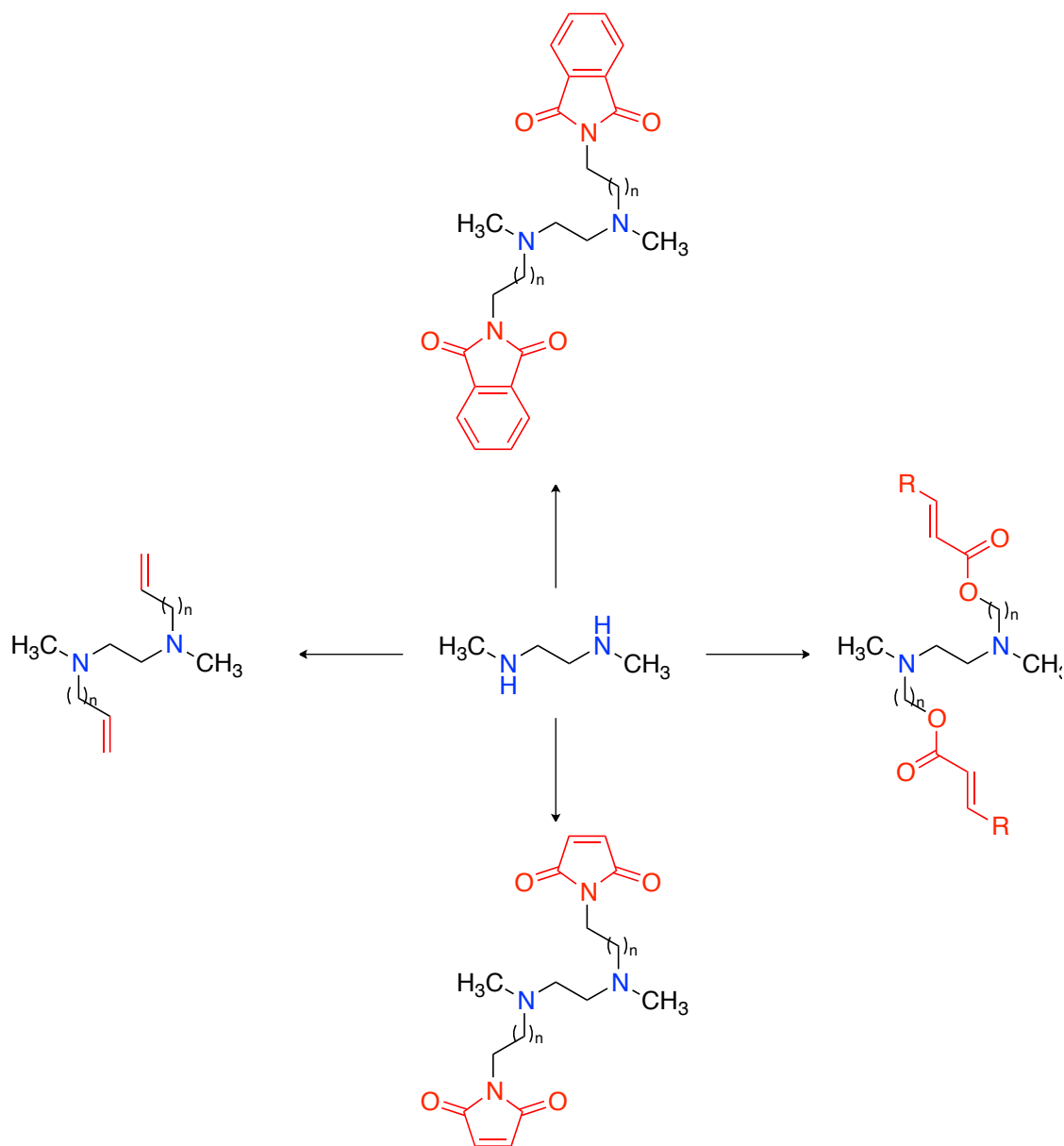


Scheme 12: Electronically responsive ligand modes of coordination

D represents a general donor (i.e. amine) that will stabilize Ni^{II} , whereas **A** represents a general π -acceptor (i.e. alkene) that will stabilize Ni^0 .

2. Results and Discussion

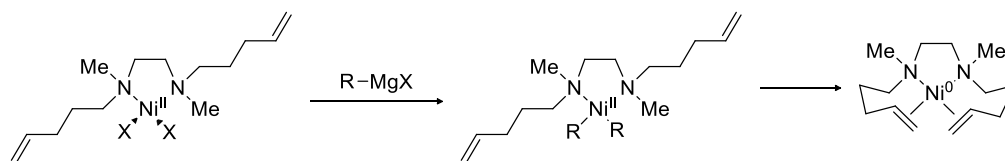
As the goal of these studies is to generate nickel complexes that are geometrically similar to palladium complexes, the first ligand requirement was to have a coordination number no higher than four. This drew us to the commercially available N,N'-dimethylethylenediamine, from which many symmetric ligands could be generated via classical routes (Scheme 13). Atoms that are hypothesized to stabilize Ni^{II} are colored blue whereas those stabilizing Ni^0 are colored red.



Scheme 13: Divergent route to functionalized diamines

2.1 Synthesis and Reactivity of NiL_2X_2 Species

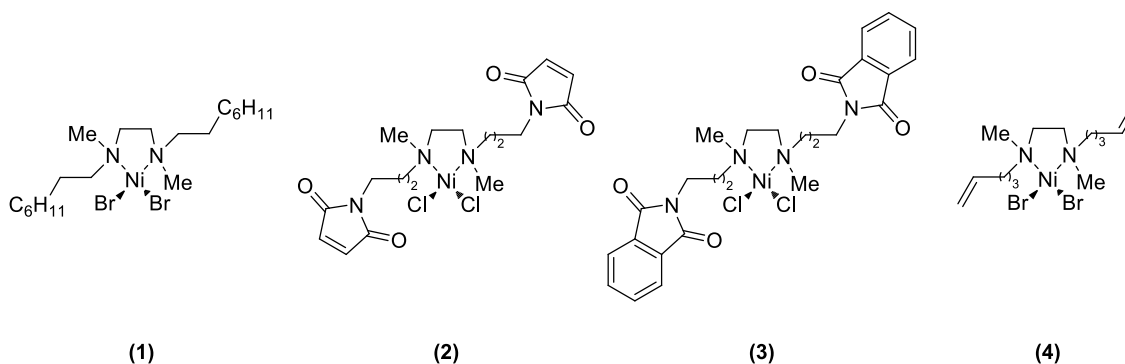
Our initial route involved isolating various $\text{Ni}^{\text{II}}\text{L}_2\text{X}_2$ complexes, followed by studying their reduction to afford the corresponding Ni^0 species. Scheme 14 displays this synthetic route.



Scheme 14: Initially proposed route to stabilized Ni⁰ complexes

A transmetallation reaction between the Ni^{II}L₂X₂ and methylmagnesium halide would afford the square planar Ni^{II}L₂(CH₃)₂, which after reductive elimination would produce ethane and a L₂Ni⁰ species. These studies would be conducted similarly to those carried out by Pörschke on (tmeda)Ni(CH₃)₂.

The following Ni^{II} complexes were synthesized and their reactivity studied:



We were first interested in examining the ability of the π-acceptors in **(2)**, **(3)**, and **(4)** to induce reductive elimination of Ni^{II}. Compound **(1)** was chosen as a negative control as it does not contain any π-accepting moieties.

Treatment of **(2)**, **(3)**, and **(4)** with methylmagnesium chloride led to the formation of nickel black and free ligand. Analyzing these reactions by mass spectrometry showed the presence of free ligand, [NiL₂(CH₃)]⁺ and [NiL₂Br]⁺, suggesting only one substitution occurred. The same transmetallation reactions were carried out in the presence of excess chlorobenzene and iodobenzene; these reactions, however, led to similar results as observed in reactions in the absence of the halobenzenes. In the event only trace amount

of a stabilized Ni^0 species was forming, one would presume the halobenzene would trap it via oxidative addition. Monitoring the progress of the transmetallation of **(1)** and **(4)** with methylmagnesium chloride via UV-Vis spectroscopy showed the disappearance of starting material and the formation of complexes possessing identical absorption spectra, suggesting both complexes form the same product (Figure 1).

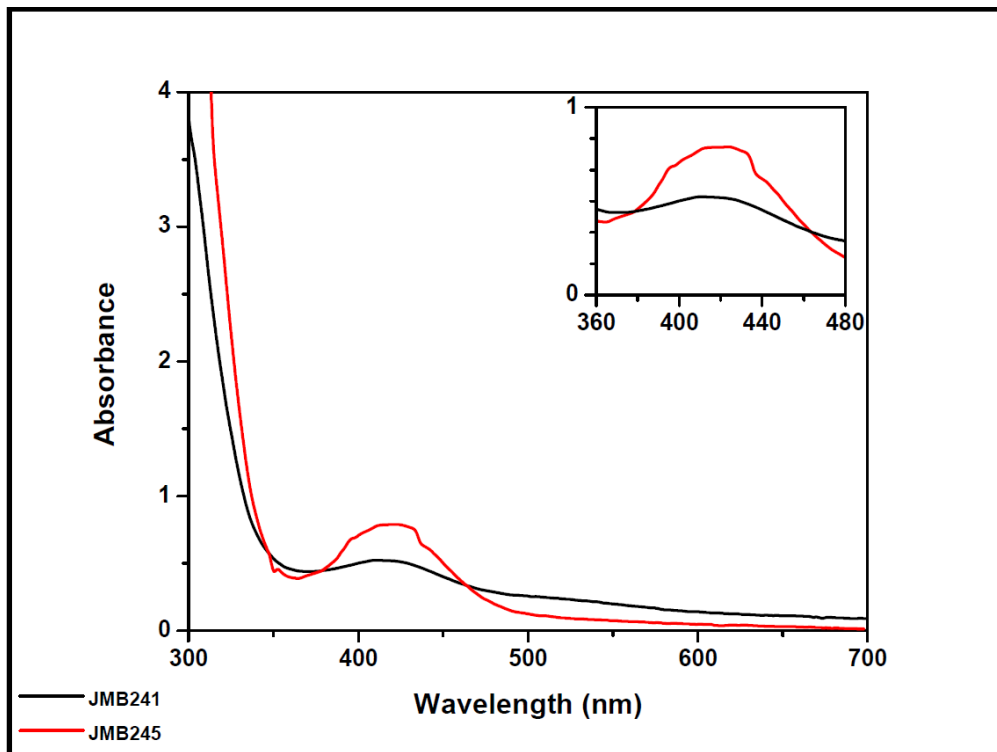


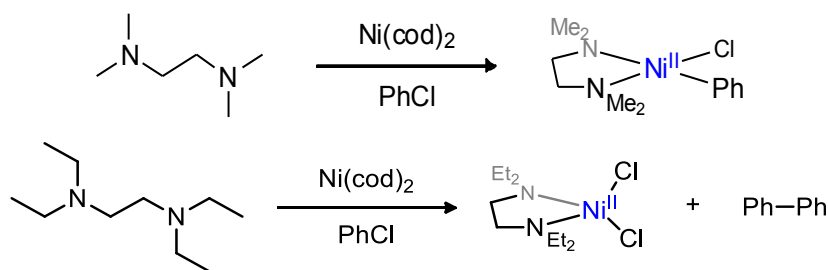
Figure 1: Transmetallation reactions of **(1)** and **(4)** with methylmagnesium chloride, as followed by UV-Vis Spectroscopy

These data suggest that generating Ni^0 complexes via the transmetallation of $\text{Ni}^{\text{II}}\text{L}_2\text{X}_2$ species with methylmagnesium chloride may not be a viable route.

2.2 Synthesis of $\text{L}_2\text{Ni}^{\text{II}}(\text{Ph})(\text{Cl})$ Species

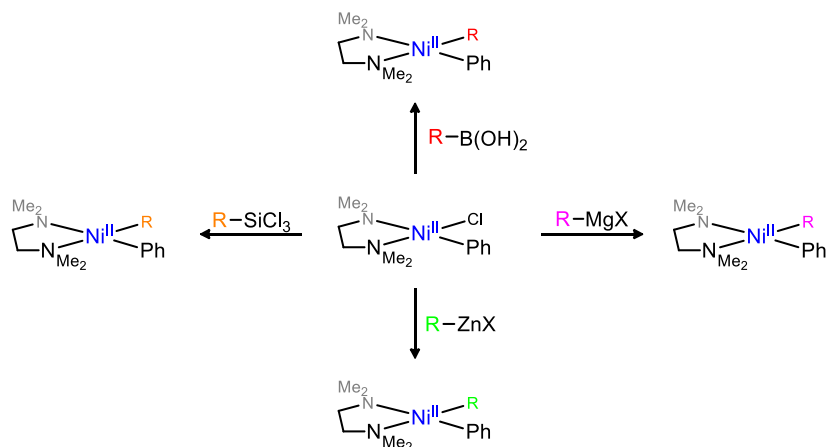
We turned our attention towards generating Ni^{II} complexes that lay on the idealized catalytic cycle (Scheme 1), as this would still provide valuable insight into reactivity similar to the isolation of Ni^0 complexes. Specifically, we aimed to generate

products that would correspond to the oxidative addition of chlorobenzene to an L_2Ni^0 species. Marshall and Grushin reported the delicate balance of sterics on reactivity as it pertained to oxidative addition reactions of nickel. In the presence of tmeda, chlorobenzene was observed to oxidatively add to $Ni(cod)_2$ to afford the square planar $(tmeda)Ni^{II}(Ph)(Cl)$. Using the same reaction conditions with teeda, instead of tmeda, the tetrahedral $(teeda)Ni^{II}Cl_2$ species is obtained (Scheme 15).²⁸



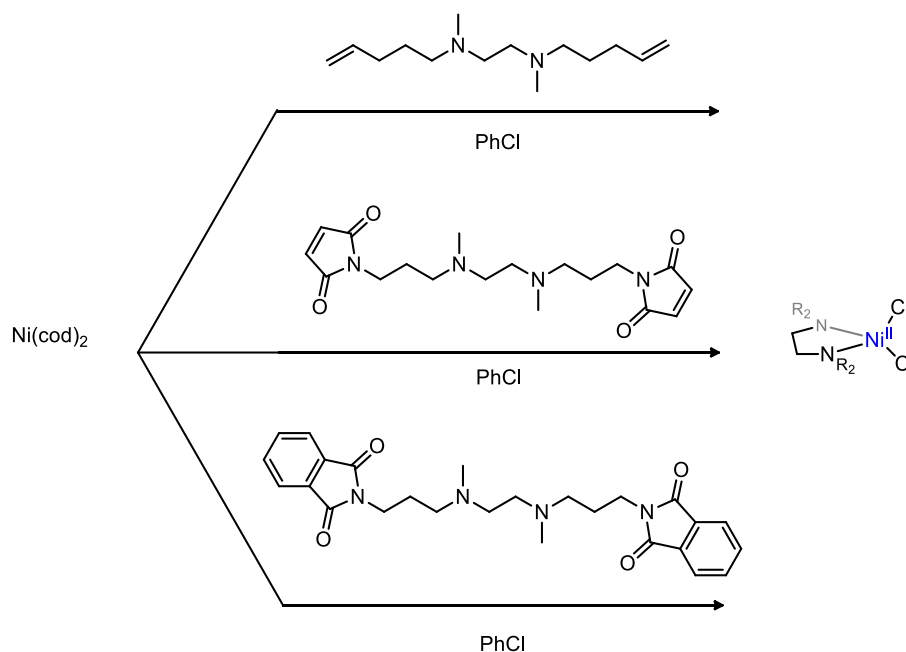
Scheme 15: Reactivity of tmeda and teeda with $Ni(cod)_2$ and PhCl

Realizing that the ligands being developed here are sterically intermediary between tmeda and teeda, we questioned which product would form in the reaction of chlorobenzene, the diamine ligand, and $Ni(cod)_2$. If the square planar $Ni^{II}L_2(Ph)(Cl)$ species could be formed, a detailed study of their reactivity could be performed (Scheme 16).



Scheme 16: Potential reactivity of Ni^{II} -aryl chloride

Scheme 17 shows the outcome of this study. Only the tetrahedral (diamine)Ni^{II}Cl₂ species was isolated.

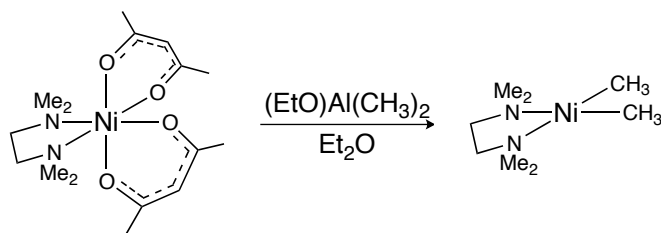


Scheme 17: Reactions of our diamine ligands with $\text{Ni}(\text{cod})_2$ and PhCl

As a result, generating the oxidative addition adducts via this route would not be feasible.

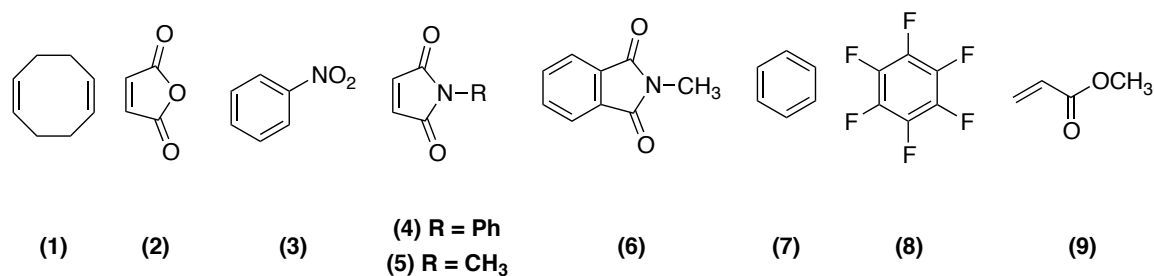
2.3 Generation of $\text{L}_2\text{Ni}^{\text{II}}(\text{CH}_3)_2$ and Intermolecular Studies

Pörschke reported the synthesis of $(\text{tmeda})\text{Ni}(\text{CH}_3)_2$ via the transmetalation of $(\text{tmeda})\text{Ni}(\text{acac})_2$ with $(\text{EtO})\text{Al}(\text{CH}_3)_2$ (Scheme 18).²⁵ We thus attempted the same synthetic route and questioned whether we could examine the effect of different π -acceptors on inducing reductive elimination. These intermolecular studies would reveal which π -accepting functional groups were required to incorporate into our ligand design, and would also expand on the study performed by Pörschke. To do so, reactions were carried out that involved the addition of an electrophile to a solution of $(\text{tmeda})\text{Ni}(\text{acac})_2$, followed by the aluminum reagent, and monitoring the reaction by UV-VIS spectroscopy.



Scheme 18: Synthesis of $(\text{tmeda})\text{Ni}(\text{CH}_3)_2$ as reported by Pörschke

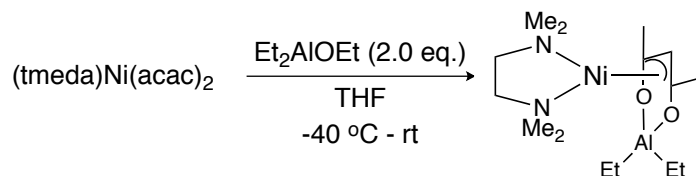
Pi-acceptors that were chosen include the following:



Using the procedure mentioned above, it was observed that **(1)**, **(6)**, **(7)**, **(8)**, and **(9)**, were unable to induce reductive elimination from Ni^{II} to afford a Ni^0 product. The inability of methyl acrylate to induce reductive elimination led to the suspicion there was a side-reaction occurring between the acrylate and the transmetalating agent, inhibiting the reaction. Because of this discrepancy, we synthesized $(\text{tmeda})\text{Ni}(\text{CH}_3)_2$ and carried out the same study.

As is reported by Pörschke, treatment of $(\text{tmeda})\text{Ni}(\text{acac})_2$ with dimethylaluminum ethoxide affords the expected $(\text{tmeda})\text{Ni}(\text{CH}_3)_2$. However, replacement of dimethylaluminum ethoxide with the commercially available diethylaluminum ethoxide led not to the expected $(\text{tmeda})\text{Ni}(\text{CH}_2\text{CH}_3)_2$, but to a stabilized Ni^0 complex (Scheme 19). Whereas $(\text{tmeda})\text{Ni}(\text{CH}_3)_2$ is an isolable complex, the inability to isolate $(\text{tmeda})\text{Ni}(\text{CH}_2\text{CH}_3)_2$ may suggest that β -hydride elimination is

occurring faster than isolation of the desired complex. No studies were conducted to assess the mechanism of decomposition of the transient $(\text{tmeda})\text{Ni}(\text{CH}_2\text{CH}_3)_2$.



Scheme 19: Generation of $(\text{tmeda})\text{Ni}(\text{acac})\text{AlEt}_2$

The product was able to be characterized by X-ray crystallography and appears as the following:

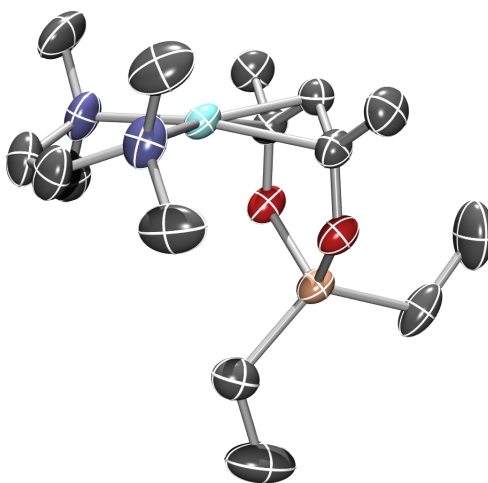
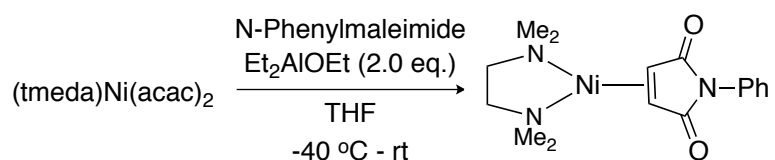


Figure 2: X-Ray crystal structure of $(\text{tmeda})\text{Ni}(\text{acac})\text{AlEt}_2$

Seeing as the overall unit cell was charge neutral implies the nickel atom to be in the zero-oxidation state. This finding opened up an avenue previously unconsidered for this project, namely that metal ions might also play a role in inducing reductive elimination of Ni^{II} . Nevertheless, this complex is interesting in that acac is behaving as a pi-acceptor, where it is typically thought of as a weak pi-donor. This shows the profound impact of the coordinated aluminum. Specifically, the aluminum ion is able to lower the LUMO of the acac ligand enough to promote an interaction with the nickel center.

Not only the aluminum-coordinated acac ligand was capable of generating an isolable Ni^0 complex, but N-phenylmaleimide also showed similar results. Treatment of a solution of N-phenylmaleimide and $(\text{tmeda})\text{Ni}(\text{acac})_2$ with the aluminum reagent led to the following transformation (Scheme 20).



Scheme 20: Generation of $(\text{tmeda})\text{Ni}(\text{N-Phenylmaleimide})$

The product was characterized by X-ray crystallography and appears as follows:

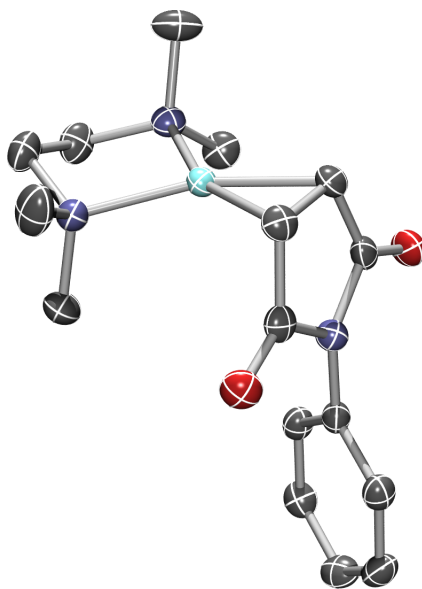


Figure 3: X-ray structure of $(\text{tmeda})\text{Ni}(\text{N-Phenylmaleimide})$

As may be seen, the nickel atom is again in the oxidation state of zero and takes on a distorted square-planar geometry. The metal is bound to the ligand through the olefinic carbons of the maleimide. The vinylic hydrogens of the maleimide moiety deviate from planarity by approximately 26° , indicating the interaction of the olefin with the metal center may be described as intermediary between olefin-coordination and a

formal metalocyclopropane. Evidence supporting this also stems from the C=C bond length in the maleimide fragment, 1.45 Å, which is quite exactly intermediary between the C-C bond length in ethane (1.54 Å) and the C=C bond length in ethylene (1.33 Å). The M-C bond lengths are 1.92 Å, the M-N bond lengths are 1.97 Å. Thus, the diamine fragment remaining bound to the electron-rich metal center may be attributed to the stronger interaction of the metal with the olefin, oxidizing the metal center enough to promote interaction with the diamine fragment.

(tmeda)Ni(CH₃)₂ was synthesized in a modified procedure from that reported by Pörschke. Interestingly, this complex is stated to be stable up to 80 °C, unless in the presence of a π-acceptor. Contrasting observations were recorded here; specifically, (tmeda)Ni(CH₃)₂ decomposes to Ni-black over the course of a few hours when standing at room temperature. Still, we were able to conduct a study on which π-acceptors may induce reductive elimination of Ni^{II}. The results of this study are shown as follows:

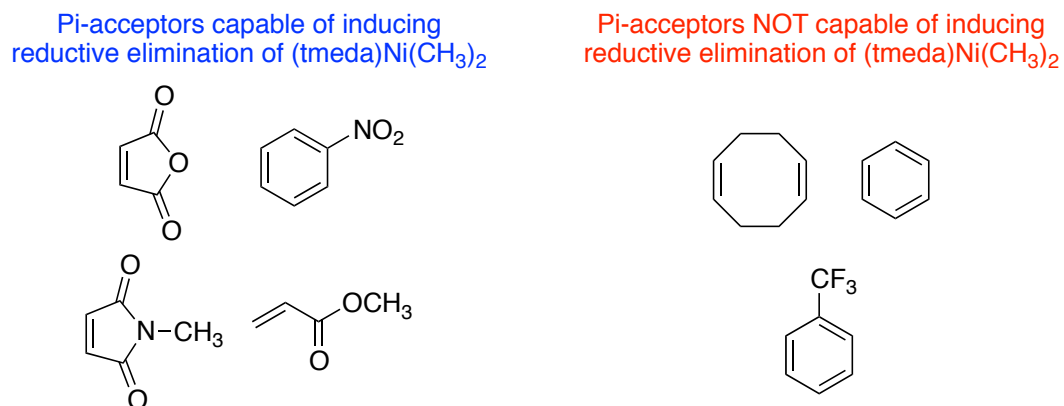


Figure 4: Results of intermolecular study with (tmeda)Ni(CH₃)₂ and various π-acceptors

As it may be seen, methyl acrylate induced reductive elimination of (tmeda)Ni(CH₃)₂. In the prior study where (tmeda)Ni(CH₃)₂ was generated *in situ*, methyl acrylate seeded

unable to induce reductive elimination. It may be inferred that dimethylaluminum ethoxide was interfering with the reaction by reacting with methyl acrylate.

Seeing these qualitative observations distinguishing the strength of a specific pi-acceptor prompted us to consider whether or not there was a measurable, quantitative requisite for the strength of the pi-acceptor. Thus, the energies of the LUMOs of the various pi-acceptors were calculated using a relatively low-level basis set and functional, SVP and BP86, using ORCA.³² The following table shows these energies (Table 1):

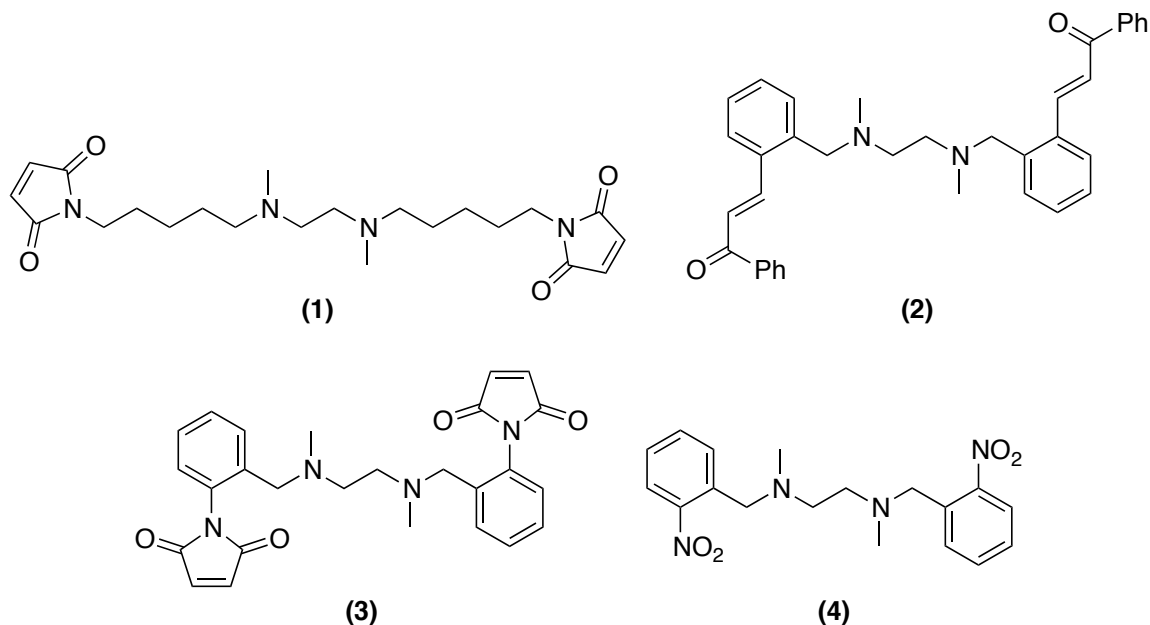
Pi-Acceptor	LUMO (eV)
Hexafluorobenzene	1.0952
Benzene	-1.0650
1,5-cyclooctadiene	-2.6241
Nitrobenzene	-3.5396
N-Methylmaleimide	-5.5758
Maleic Anhydride	-6.1078

Table 1: Calculated LUMO energies of various π -acceptors. Those in bold have been shown to induce reductive elimination of ethane from [(tmeda)Ni^{II}(CH₃)₂] (Figure 3).

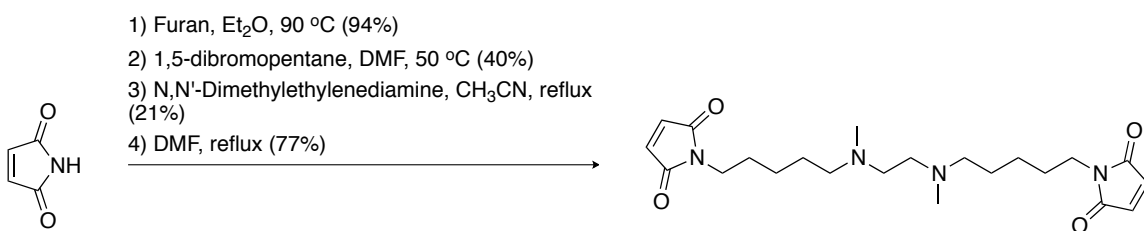
While these calculations merely provide estimates of the various LUMO energies, and an exact energy threshold has not been determined, one clear correlation is the π -acceptors bearing the lowest energy LUMO do induce reductive elimination of (tmeda)Ni^{II}(CH₃)₂. It would also be of interest to tabulate the LUMO energies of various M(acac)₂ salts.

2.4 Ligand Development

It seemed evident from these data that the ideal ligand should be comprised of a nitroarene, enone, or a maleimide with a symmetric diamine scaffold. With the help of molecular mechanics simulations carried out on Argus, we chose the following diamines as ligands to be studied:

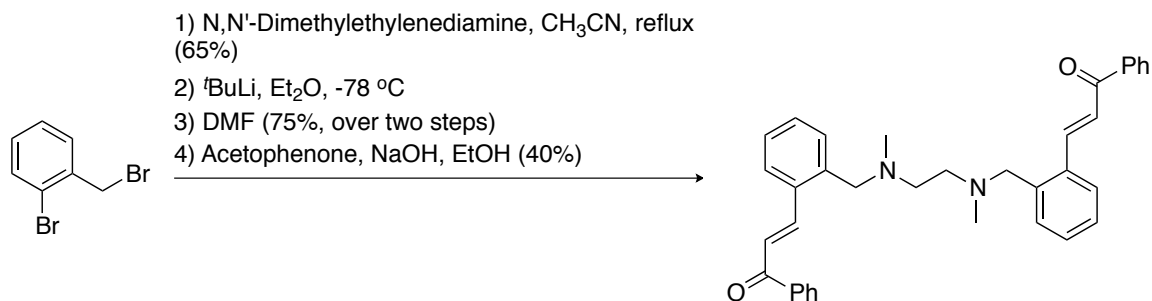


As may be seen, the four ligands shown above all contain the central diamine scaffold with a tethered π -acceptor. These ligands may all be synthesized via classic organic transformations. Ligands (1), (2), (3), and (4) may be synthesized as depicted in the following schemes:



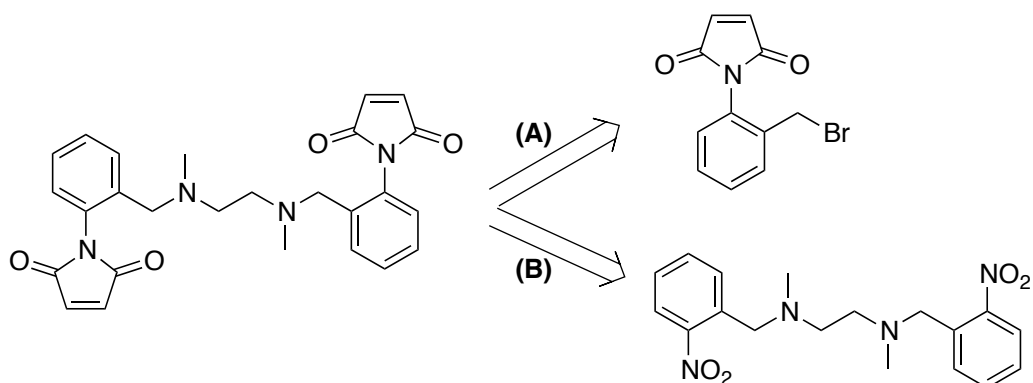
Scheme 21: Synthesis of ligand (1)

A Diels-Alder reaction between maleimide and furan furnishes the protected maleimide moiety, which may then be alkylated with the appropriate dihaloalkane, aminated with the core diamine, and finally deprotected to afford the ligand. Initial attempts at simply alkylating maleimide with the required dihaloalkane were unsuccessful. As a result, other routes were explored. Optimization of the amination and retro Diels-Alder reactions remains to be done. Ligand (2) is synthesized according to the following scheme:



Scheme 22: Synthesis of ligand (2)

Amination of commercially available 2-bromobenzyl bromide followed by a halogen-metal exchange, formylation, and aldol condensation furnishes the ligand. Ligand (3), though desired, has proven to be the most difficult to synthesize. The attempted synthetic routes are shown in the following scheme:



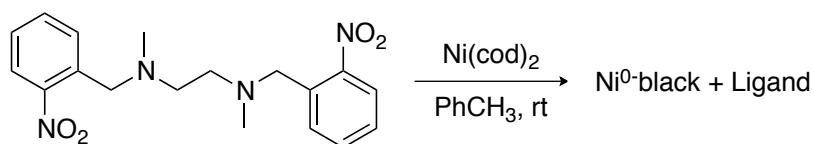
Scheme 23: Synthetic strategy towards ligand (3)

The synthon shown in path (A) has presented difficulties associated with its synthesis. Generating the maleimide from *o*-toluidine is successful, however benzylic bromination with both N-bromosuccinimide as well as Br₂ afforded complex mixtures. Pathway (B), which possesses ligand (4) as a synthon, involves the reduction of the nitroarene to the corresponding aniline followed by maleimide generation. Reduction of the nitroarene by

treatment with Sn-powder and HCl afforded trace amount of product, similar results obtained with a Pd/C catalyzed reduction. One issue may stem from the ability of both the nitroarene and corresponding aniline to bind palladium, in either the reduced or oxidized form. Ligand (**4**) is synthesized in one step from the commercially available 2-nitrobenzyl bromide and N,N'-dimethylethylenediamine.

3. Preliminary Metallation Studies

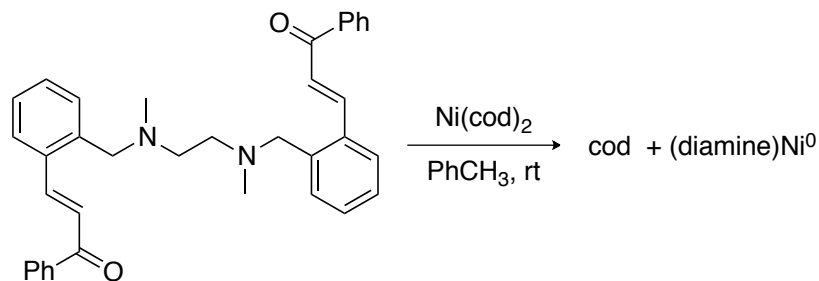
Progress has been made to study the metallation of the diamine ligands mentioned in the previous section. When the diamine with a pendant nitroarene is treated with one equivalent of Ni(cod)₂, the formation of nickel-black is observed instantly (Scheme 24).



Scheme 24: Metallation of diamine containing pendant nitroarene

Following the reaction by ¹H NMR spectroscopy further confirms this. Upon addition of a solution of Ni(cod)₂ in C₆D₆ to a solution of the diamine in C₆D₆, the formation of free cod is observed, in addition to free ligand. No changes were observed in chemical shifts of the diamine. This suggests that the ligand may be accelerating the rate of decomposition of Ni(cod)₂ to nickel-black.

In contrast, when the diamine containing the pendant chalcone is treated with Ni(cod)₂, a ligand exchange is occurring (Scheme 25).



Scheme 25: Metallation of diamine containing pendant chalcone

^1H NMR spectroscopic analysis of the same reaction in C_6D_6 indicates a shift in the vinylic protons from about 8.20 ppm to about 6.20 ppm, the formation of free cod, and a decrease in overall symmetry. It appears only one of the enone moieties may be coordinating to the nickel center, which is analogous to the mode of coordination in the previously mentioned $(\text{tmeda})\text{Ni}(\text{N-Phenylmaleimide})$. The product of this reaction remains to be further characterized.

4. Conclusions

In conclusion, an investigation into the development of a novel class of ligands has been undertaken that aims for the stabilization of two, diamagnetic oxidation states of nickel. We have targeted diamines derived from the commercially available N,N'-dimethylethylenediamine containing pendant nitroarenes, maleimides, and chalcones. Ligands have been generated and their metallation studied, however only with preliminary data. Challenges associated with the maleimide-containing ligands were associated with the synthesis, and remains to be optimized. Attempts at generating complexes bearing a coordinated nitroarene resulted in the irreversible formation of nickel black and free ligand. However, a successful ligand exchange may be occurring with the diamine containing a pendant chalcone, though this product remains to be fully

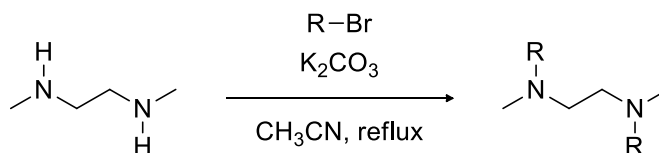
characterized. Future work will include focus on generating and isolating Ni⁰ complexes bearing diamines with tethered π -acceptors, as well as studying their reactivity.

5. Experimental Section

General Experimental

All reactions were carried out in oven-dried glassware under an inert atmosphere of dry nitrogen utilizing standard Schlenk techniques or conducted in an MBraun Glovebox, unless noted otherwise. Reagents were used as received from commercial suppliers. Acetonitrile, dichloromethane, diethyl ether, pentane, and toluene were obtained from drying columns (Grubbs type solvent purifier). ^1H NMR spectra were recorded on Varian and INOVA NMR spectrometers at 600 or 400 MHz. Tetramethylsilane (TMS) was used as an internal standard ($\delta = 0.00$ ppm). NMR data are reported as follows: chemical shift, multiplicity (s = singlet, d = doublet, t = triplet, q = quartet, p = pentet, m = multiplet) and coupling constants in Hz. ^{13}C NMR spectra were recorded on Varian and INOVA NMR spectrometers at 100 or 150 MHz using the solvent CDCl_3 as an internal standard ($\delta = 77.0$ ppm) and were carried out with proton decoupling. Mass spectral determinations were recorded at the Mass Spectrometry Center at Emory University on a JEOL JMS-SX102/SX102A/E mass spectrometer. Elemental analyses were carried out by Atlantic Microlabs, Inc, Norcross, Georgia. UV-Vis spectra were recorded on a Shimadzu UV-3600 spectrometer.

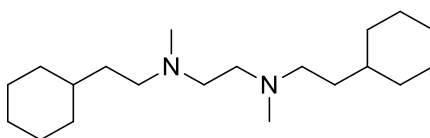
General Procedure for the Dialkylation of N,N'-Dimethylethylenediamine



To an oven-dried round bottom flask was added CH_3CN , K_2CO_3 , N,N'-Dimethylethylenediamine, and the alkyl bromide. The mixture was heated to reflux (82 °C) overnight. The mixture was then cooled to room temperature and was quenched with

aqueous saturated NaHCO_3 (50 mL / g of diamine). The biphasic solution was extracted with Et_2O (100 mL / g of diamine). The aqueous layer was discarded and the organic layer was washed with HCl (2N) until the new aqueous layer had a $\text{pH} < 3$. The aqueous layer was isolated and extracted with Et_2O (20 mL / g of diamine) to remove any organic impurities. Solid KOH was then added until the aqueous layer reached $\text{pH} > 10$, and Et_2O (100 mL / g of diamine) was then added to extract. The organic layer was dried (MgSO_4), filtered, and concentrated under reduced pressure to afford the title compound. No further purification was necessary.

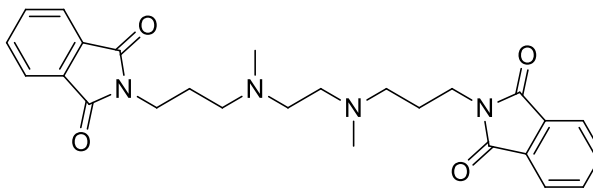
N1,N2-bis(2-cyclohexylethyl)-N1,N2-dimethylethane-1,2-diamine



Synthesized from CH_3CN (100 mL), K_2CO_3 (3.62 g, 26.1 mmol, 3.0 eq.), $\text{N,N}'$ -Dimethylethylenediamine (770 mg, 0.93 mL, 8.7 mmol, 1.0 eq.), and (2-Bromoethyl)cyclohexane (5.00 g, 26.1 mmol, 3.0 eq.). Yield: Light yellow liquid, 1.05 g (39%).

^1H NMR (400 MHz, CDCl_3) δ 2.38 (s, 4H), 2.34 – 2.31 (t, $J = 6.8$ Hz, 4H), 2.16 (s, 6H), 1.71 – 1.62 (m, 10H), 1.34 – 1.13 (m, 12H), 0.94 – 0.86 (m, 4H). ^{13}C NMR (100 MHz, CDCl_3) δ 57.2, 57.1, 43.8, 37.3, 36.3, 34.9, 28.0, 27.7. HRMS (APCI) Calcd for $\text{C}_{20}\text{H}_{41}\text{N}_2$ (M+H): 309.3264. Found: 309.3266.

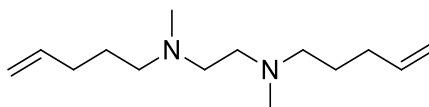
2,2'-((ethane-1,2-diylbis(methylazanediyl))bis(propane-3,1-diyl))bis(isoindoline-1,3-dione)



Synthesized from CH_3CN (50 mL), K_2CO_3 (9.41 g, 68.1 mmol, 6.0 eq.), $\text{N,N}'$ -Dimethylethylenediamine (1.00 g, 1.22 mL, 11.3 mmol, 1.0 eq.), and N -(3-Bromopropyl)phthalimide (7.60 g, 28.4 mmol, 2.5 eq.). Yield: White solid, 3.45 g (66%).

^1H NMR (400 MHz, CDCl_3) δ 7.85 – 7.83 (dd, $J = 5.6$ Hz, $J = 3.2$ Hz, 4H), 7.72 – 7.69 (dd, $J = 5.6$ Hz, $J = 3.2$ Hz, 4H), 3.74 – 3.70 (t, $J = 7.2$ Hz, 4H), 2.43 – 2.41 (m, 4H), 2.20 (s, 6H), 2.05 (s, 4H), 1.87 – 1.80 (m, 4H). ^{13}C NMR (100 MHz, CDCl_3) δ 168.3, 133.8, 132.1, 123.1, 55.6, 55.4, 42.3, 36.3, 26.2. HRMS (APCI) Calcd for $\text{C}_{26}\text{H}_{31}\text{O}_4\text{N}_4$ ($\text{M}+\text{H}$): 463.2339. Found: 463.2339.

N1,N2 -dimethyl- N1,N2 -di(pent-4-en-1-yl)ethane-1,2-diamine

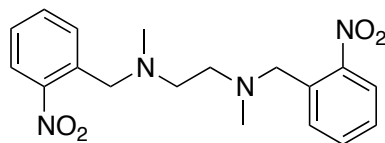


Synthesized from CH_3CN (100 mL), K_2CO_3 (5.83 g, 42.2 mmol, 3.0 eq.), $\text{N,N}'$ -Dimethylethylenediamine (1.24 g, 1.50 mL, 14.1 mmol, 1.0 eq.), and 5-Bromo-1-pentene (6.29 g, 5.00 mL, 42.2 mmol, 3.0 eq.). Yield: Light yellow liquid, 0.67 g (21%).

^1H NMR (600 MHz, CDCl_3) δ 5.85 – 5.78 (m, 2H), 5.03 – 5.00 (dd, $J = 16.8$ Hz, $J = 1.2$ Hz, 2H), 4.96 – 4.94 (m, 2H), 2.47 (s, 4H), 2.37 – 2.34 (t, $J = 7.4$ Hz, 4H), 2.24 (s, 6H), 2.07 – 2.04 (m, 4H), 1.59 – 1.54 (m, 4H). ^{13}C NMR (150 MHz, CDCl_3) δ 138.6, 114.5,

57.8, 55.6, 42.7, 31.6, 26.4. HRMS (APCI) Calcd for $C_{14}H_{29}N_2$ (M+H): 225.2325. Found: 225.2324.

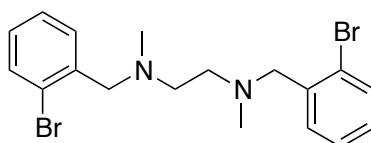
***N*¹,*N*²-dimethyl-*N*¹,*N*²-bis(2-nitrobenzyl)ethane-1,2-diamine**



Synthesized from CH_3CN (200 mL), K_2CO_3 (9.64 g, 69.78 mmol, 2.5 eq.), *N,N'*-Dimethylethylenediamine (2.46 g, 3.00 mL, 27.91 mmol, 1.0 eq.), and 2-Nitrobenzyl bromide (9.64 g, 69.78 mmol, 2.5 eq.). Yield: Light yellow solid, 9.33 g (93%).

1H NMR (400 MHz, $CDCl_3$) δ 7.83 – 7.81 (dd, $J = 8.4$ Hz, $J = 1.2$ Hz, 2H), 7.65 – 7.63 (d, $J = 7.6$ Hz, 2H), 7.55 – 7.51 (td, $J = 7.6$ Hz, $J = 1.2$ Hz, 2H), 7.40 – 7.36 (td, $J = 9.2$ Hz, $J = 1.2$ Hz, 2H), 3.79 (s, 4H), 2.52 (s, 4H), 2.16 (s, 6H). ^{13}C NMR (100 MHz, $CDCl_3$) δ 149.6, 134.9, 132.5, 130.9, 127.7, 124.3, 58.9, 55.5, 42.6. HRMS (APCI) Calcd for $C_{18}H_{23}O_4N_4$ (M+H): 359.1714. Found: 359.1716.

***N*¹,*N*²-bis(2-bromobenzyl)-*N*¹,*N*²-dimethylethane-1,2-diamine**

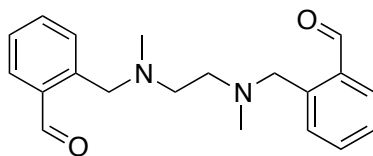


Synthesized from CH_3CN (200 mL), K_2CO_3 (16.6 g, 120 mmol, 3.0 eq.), *N,N'*-Dimethylethylenediamine (3.52 g, 4.30 mL, 40. mmol, 1.0 eq.), and 2-Bromobenzyl bromide (25.0 g, 100 mmol, 2.5 eq.). Yield: Clear liquid, 10.58 g (65%).

^{13}C NMR (100 MHz, CDCl_3) δ 138.4, 132.6, 130.8, 128.3, 121.2, 124.5, 61.7, 55.8, 42.8.

HRMS (APCI) Calcd for $\text{C}_{18}\text{H}_{23}\text{Br}_2\text{N}_2$ (M+H): 425.0223. Found: 425.0223.

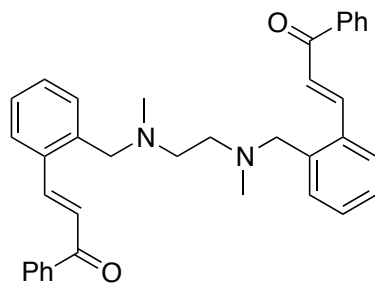
2,2'-((ethane-1,2-diylbis(methylazanediyl))bis(methylene))dibenzaldehyde



A 500 mL round bottom flask was charged with N^1,N^2 -bis(2-bromobenzyl)- N^1,N^2 -dimethylethane-1,2-diamine (10.88 g, 25.53 mmol, 1.0 eq.) and Et_2O (200 mL). The flask was cooled to -78° and $t\text{BuLi}$ (1.7M in pentane, 60 mL, 102.1 mmol, 4.0 eq.) was added. The reaction stirred, while cold, for 3 h. DMF (7.46 g, 8.1 mL, 102.1 mmol, 4.0 eq.) was added and the reaction was allowed to warm to room temperature. After 5 h, the reaction was quenched with H_2O (50 mL). The organic layer was washed with H_2O (50 mL), dried (Na_2SO_4), and concentrated to yield the desired product as a colorless liquid (5.78 g, 75%).

^1H NMR (400 MHz, CDCl_3) δ 10.39 (s, 2H), 7.86 – 7.84 (dd, $J = 7.2$ Hz, $J = 1.2$ Hz, 2H), 7.52 – 7.48 (td, $J = 7.2$ Hz, $J = 1.6$ Hz, 2H), 7.42 – 7.35 (m, 4H), 3.79 (s, 4H), 2.55 (s, 4H), 2.14 (s, 6H). ^{13}C NMR (100 MHz, CDCl_3) δ 192.4, 141.8, 134.9, 133.2, 130.5, 129.4, 127.7, 59.6, 54.9, 42.1. HRMS (APCI) Calcd for $\text{C}_{20}\text{H}_{24}\text{O}_2\text{N}_2$ (M+H): 325.1911. Found: 325.1913.

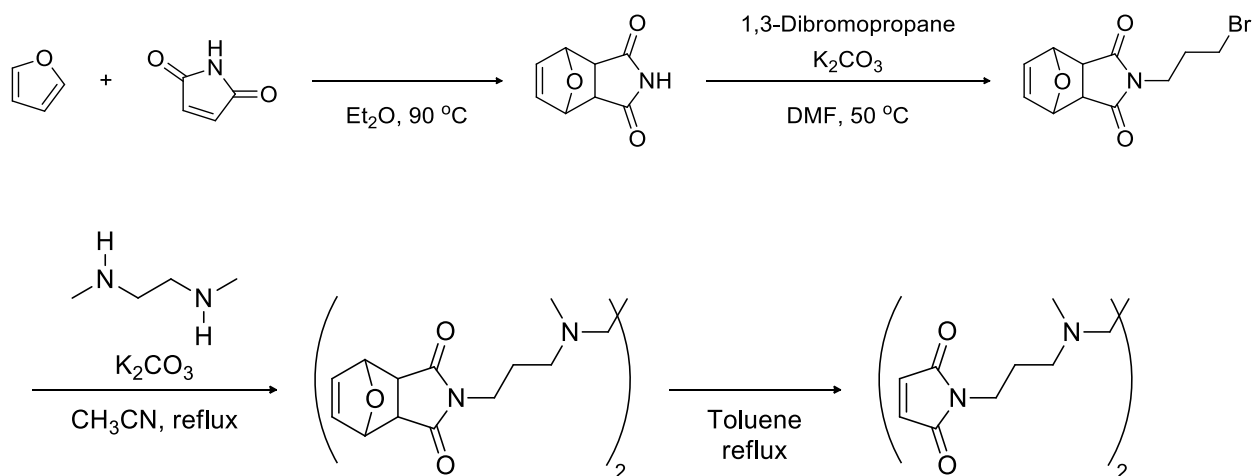
(2E,2'E)-3,3'-(((ethane-1,2-diylbis(methylazanediyl))bis(methylene))bis(2,1-phenylene))bis(1-phenylprop-2-en-1-one)



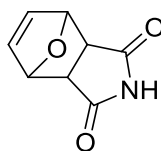
A 250 mL round bottom flask was charged with 2,2'-((ethane-1,2-diylbis(methylazanediy))bis(methylene))dibenzaldehyde (5.44 g, 16.76 mmol, 1.0 eq), ethanol (15 mL), NaOH (10%, w/v, 20 mL). Acetophenone (4.02 g, 3.91 mL, 33.53 mmol, 2.0 eq.) was added and the reaction stirred at room temperature. After 1 d, the reaction was partitioned between EtOAc (300 mL) and H₂O (100 mL). The organic layer was dried (Na₂SO₄) and concentrated. The crude product was purified by flash chromatography using EtOAc / Et₃N / Hexanes (1 / 1 / 10, v/v) eluent to afford the desired product as a yellow solid (3.22 g, 40%).

¹H NMR (400 MHz, CDCl₃) δ 8.27 – 8.23 (d, *J* = 16.0 Hz, 1H), 7.99 – 7.96 (m, 2H), 7.70 – 7.68 (t, *J* = 5.6 Hz, 1H), 7.58 – 7.53 (t, *J* = 6.4 Hz, 1H), 7.49 – 7.46 (t, *J* = 7.6 Hz, 2H), 7.37 – 7.33 (d, *J* = 16.0 Hz, 1H), 7.32 – 7.25 (m, 4H), 3.57 (s, 2H), 2.55 (s, 2H), 2.15 (s, 3H). ¹³C NMR (100 MHz, CDCl₃) δ 191.1, 143.1, 139.2, 138.3, 134.7, 132.5, 130.8, 129.8, 128.6, 128.5, 127.5, 126.6, 123.3, 60.4, 55.1, 42.4. HRMS (APCI) Calcd for C₃₆H₃₆O₂N₂ (M+H): 529.2850. Found: 529.2851.

General Route to 1,1'-((ethane-1,2-diylbis(methylazanediy))bis(propene-3,1-diyl))bis(1H-pyrrole-2,5-dione)



3a,4,7,7a-tetrahydro-1H-4,7-epoxyisoindole-1,3(2H)-dione



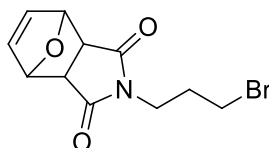
Procedure followed from: *Chem. Bio. Chem.*, **2008**, *9*, 552.

A 420 mL heavy wall, pressure vessel was charged with Et₂O (175 mL), maleimide (5.0 g, 57.5 mmol, 1.0 eq.), and furan (19.0 mL, 257 mmol, 4.5 eq.). The mixture was heated to 90 °C for 2 days. The vessel was allowed to cool down and the white solid was collected by vacuum filtration. Yield: 8.00 g (94%).

¹H NMR (400 MHz, CDCl₃) δ 8.17 (s, 1H), 6.53 (s, 2H), 5.32 (s, 2H), 2.90 (s, 2H).

Data are consistent with the literature: *Tetrahedron Lett.*, **2006**, *47*, 7213. *Chem. Bio. Chem.*, **2008**, *9*, 552.

2-(3-bromopropyl)-3a,4,7,7a-tetrahydro-1H-4,7-epoxyisoindole-1,3(2H)-dione



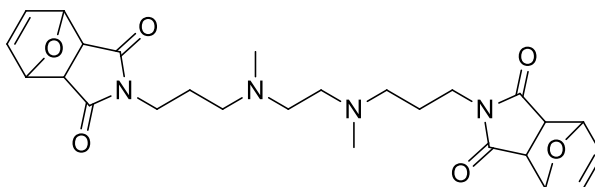
Procedure followed from: *Chem. Bio. Chem.*, **2008**, *9*, 552.

1,3-Dibromopropane (39.6 g, 20.0 mL, 196 mmol, 2.0 eq.) was added to a suspension of K_2CO_3 (33.9 g, 245 mmol, 2.5 eq.), DMF (400 mL), and 3a,4,7,7a-tetrahydro-1H-4,7-epoxyisindole-1,3(2H)-dione (16.2 g, 98.0 mmol, 1.0 eq.). The suspension was heated to 50 °C for 2 h and was then concentrated under reduced pressure. The residue was partitioned between EtOAc / H_2O (300 mL / 100 mL) and the organic layer was dried ($MgSO_4$) and concentrated under reduced pressure. The crude product was purified by flash column chromatography using EtOAc / hexane (30%, v/v) eluent to afford the title compound as a white solid. Yield: 11.0 g (40%).

1H NMR (400 MHz, $CDCl_3$) δ 6.53 (s, 2H), 5.27 (s, 2H), 3.65 – 3.62 (dd, $J = 6.8$ Hz, $J = 7.2$ Hz, 2H), 3.36 – 3.33 (dd, $J = 6.8$ Hz, $J = 6.4$ Hz, 2H), 2.86 (s, 2H), 2.18 – 2.12 (m, 2H).

Data are consistent with the literature: *Chem. Bio. Chem.*, **2008**, *9*, 552.

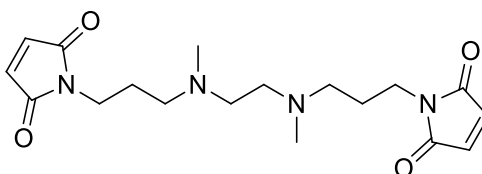
2,2'-((ethane-1,2-diylbis(methylazanediyl))bis(propane-3,1-diyl))bis(3a,4,7,7a-tetrahydro-1H-4,7-epoxyisindole-1,3(2H)-dione)



An oven dried, 250 mL round bottom flask was charged with 2-(3-bromopropyl)-3a,4,7,7a-tetrahydro-1H-4,7-epoxyisoindole-1,3(2H)-dione (4.0 g, 14.0 mmol, 2.0 eq.), CH₃CN (100 mL), K₂CO₃ (2.12 g, 15.4 mmol, 2.2 eq.), and N,N'-Dimethylethylenediamine (616 mg, 0.75 mL, 6.99 mmol, 1.0 eq.). The mixture was heated to reflux (82 °C). After 12 h, the mixture cooled to room temperature and was then partitioned between EtOAc / H₂O (200 mL / 100 mL) and the organic layer was washed with H₂O (20 mL), dried (MgSO₄), and concentrated to afford the title compound as a white solid. Yield: 0.74 g (21%).

¹H NMR (400 MHz, CDCl₃) δ 6.51 (s, 4H), 5.26 (s, 4H), 3.53 – 3.49 (t, *J* = 7.2 Hz, 4H), 2.83 (s, 4H), 2.41 (s, 4H), 2.37 – 2.33 (dd, *J* = 6.8 Hz, *J* = 7.6 Hz, 4H), 2.20 (s, 6H), 1.76 – 1.68 (m, 4H). ¹³C NMR (100 MHz, CDCl₃) δ 176.2, 136.5, 80.9, 55.4, 55.2, 47.3, 42.3, 37.3, 25.2. HRMS (APCI) Calcd for C₂₆H₃₅N₄O₆ (M+H): 499.2551. Found: 499.2552.

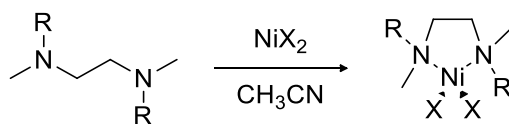
1,1'-((ethane-1,2-diylbis(methylazanediyl))bis(propane-3,1-diyl))bis(1H-pyrrole-2,5-dione)



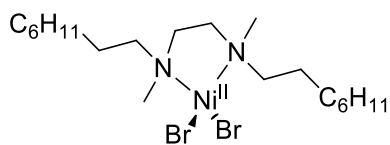
2,2'-((ethane-1,2-diylbis(methylazanediyl))bis(propane-3,1-diyl))bis(3a,4,7,7a-tetrahydro-1H-4,7-epoxyisoindole-1,3(2H)-dione) (156 mg, 0.311 mmol) was dissolved in 10 mL of toluene and heated to reflux (110 °C). After 1 d, the reaction was filtered into a 20 mL scintillation vial and concentrated to afford the title product as a light-yellow solid (100 mg,

^1H NMR (400 MHz, CDCl_3) δ 6.69 (s, 4H), 3.58 – 3.54 (t, $J = 7.2$ Hz, 4H), 2.41 (s, 4H), 2.38 – 2.35 (t, $J = 7.2$ Hz, 4H), 2.20 (s, 6H), 1.78 – 1.71 (m, 4H). ^{13}C NMR (100 MHz, CDCl_3) δ 170.8, 134.0, 55.4, 55.4, 42.3, 36.2, 26.1. HRMS (APCI) Calcd for $\text{C}_{18}\text{H}_{27}\text{N}_4\text{O}_4$ (M+H): 363.2027. Found: 363.2028.

General Procedure for Metallation of 1,2-diamine:



A round bottom flask was charged with CH_3CN and the diamine ligand. To this solution was added the NiX_2 in one quantity. The solution quickly became deep purple and was stirred at room temperature. Insoluble impurities were removed via filtration and the resulting purple solution was concentrated under vacuum. The Ni^{II} -complex was purified via recrystallization from hot toluene or by vapor diffusion (Pentane into a concentrated CH_2Cl_2 solution)



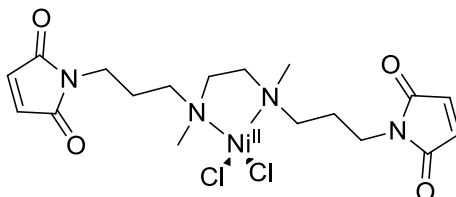
1

A 250 mL round bottom flask was charged with CH_3CN (100 mL) and the diamine ligand (500 mg, 1.62 mmol, 1.0 eq.). To this solution was added $\text{NiBr}_2 \cdot \text{H}_2\text{O}$ (708 mg, 3.24 mmol, 2.0 eq.) in one portion. After 12 h, the reaction was filtered into a 250 mL round bottom flask and the resulting purple solution was concentrated. The solid was

crystallized from hot toluene (10 mL) to produce deep purple crystals. Yield: 300 mg (35%).

HRMS (ESI): $m/z = 523.1863$ (M-H)⁺

Anal. Calcd for C₂₀H₄₀Br₂N₂Ni: C, 45.58; H, 7.65; N, 5.32. Found: C, 45.64; H, 7.55; N, 5.30.



2

A 100 mL round bottom flask was charged with CH₃CN (40 mL) and the diamine ligand (109 mg, 0.30 mmol, 1.0 eq.). To this solution was added NiCl₂ • 6H₂O (107 mg, 0.451 mmol, 1.5 eq.) in one portion. After 15 h, the reaction was filtered into a 100 mL round bottom flask and concentrated. The residue was crystallized by vapor diffusion of pentane into a concentrated dichloromethane solution to afford deep purple crystals. Yield: 100 mg (75%).

HRMS (ESI) Calcd for C₁₈H₂₆O₄N₄ClNi (M-Cl): 455.0991. Found: 455.0992.

Anal. Calcd for C₁₈H₂₆Cl₂N₄NiO₄: C, 43.94; H, 5.33; N, 11.39. Found: C, 43.96; H, 5.40; N, 11.33.



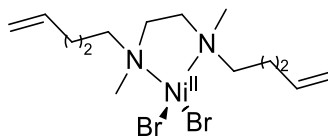
3

A 250 mL round bottom flask was charged with CH₃CN (60 mL) and the diamine ligand (1.0 g, 2.16 mmol, 1.0 eq.). To this solution was added NiCl₂ • 6H₂O (770 mg, 3.24 mmol, 1.5 eq.) in one portion. After 15 h, the reaction was filtered into a 250 mL round bottom flask and concentrated. The residue was crystallized by vapor diffusion of pentane into a concentrated dichloromethane solution to afford deep purple crystals. Yield: 500 mg (42%).

HRMS (ESI) Calcd for C₂₆H₃₀O₄N₄ClNi (M-Cl): 555.1304. Found: 555.1306.

Anal. Calcd for C₂₆H₃₀Cl₂N₄NiO₄: C, 52.74; H, 5.11; N, 9.46. Found: C, 52.76; H, 5.21; N, 9.32.

X-ray crystallographic information is at the end of this document.



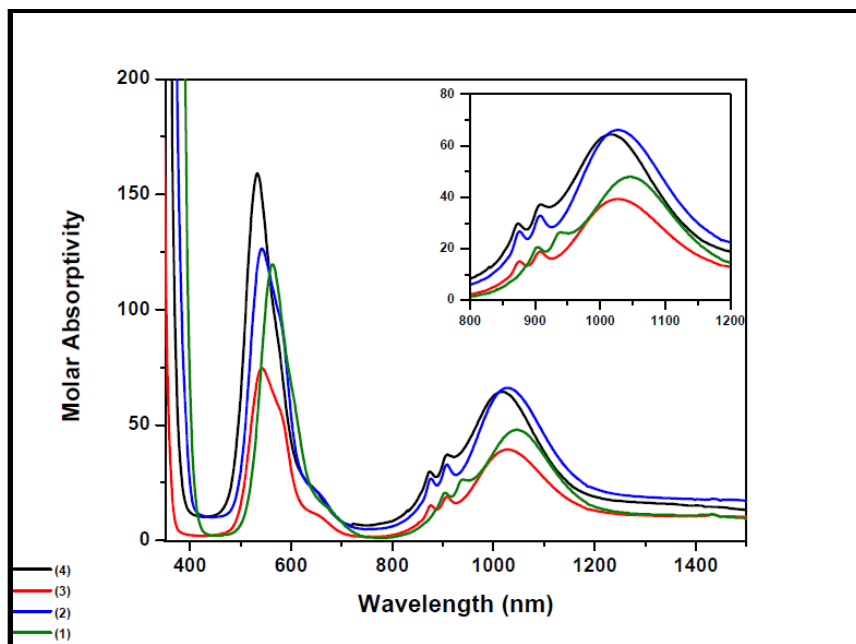
4

A 250 mL round bottom flask was charged with CH₃CN (100 mL) and the diamine ligand (500 mg, 2.2 mmol, 1.0 eq.). To this solution was added NiBr₂ • H₂O (970 mg, 4.5 mmol, 2.0 eq.) in one portion. After 19 h, the reaction was filtered into a 250 mL round bottom flask and the resulting purple solution was concentrated. The solid was recrystallized from hot toluene (10 mL) to produce deep purple crystals. Yield: 400 mg (41%).

HRMS (ESI) Calcd for C₁₄H₂₈N₂BrNi (M-Br): 361.0784. Found: 361.0786.

Anal. Calcd for $C_{14}H_{28}Br_2N_2Ni$: C, 37.97; H, 6.37; N, 6.33. Found: C, 38.14; H, 6.48; N, 6.25.

X-ray crystallographic information is at the end of this document.

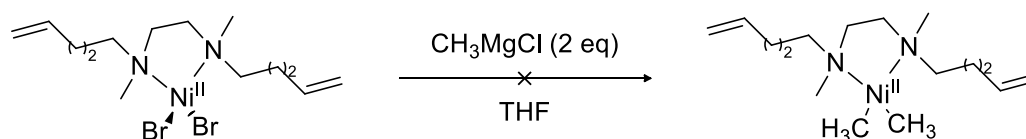


UV-Vis of Ni^{II} complexes **1**, **2**, **3**, **4**

Compound	λ_{max} (nm)	ϵ ($L \times mol^{-1} \times cm^{-1}$)
1	562, 904, 940, 1046	120, 20.5, 26.3, 47.9
2	542, 876, 908, 1027	127, 26.7, 32.8, 66.1
3	542, 876, 908, 1027	74.7, 15.1, 18.9, 39.3
4	532, 874, 909, 1016	159, 29.8, 37.2, 64.3

Additions of CH_3MgCl to NiL_2X_2 complexes:

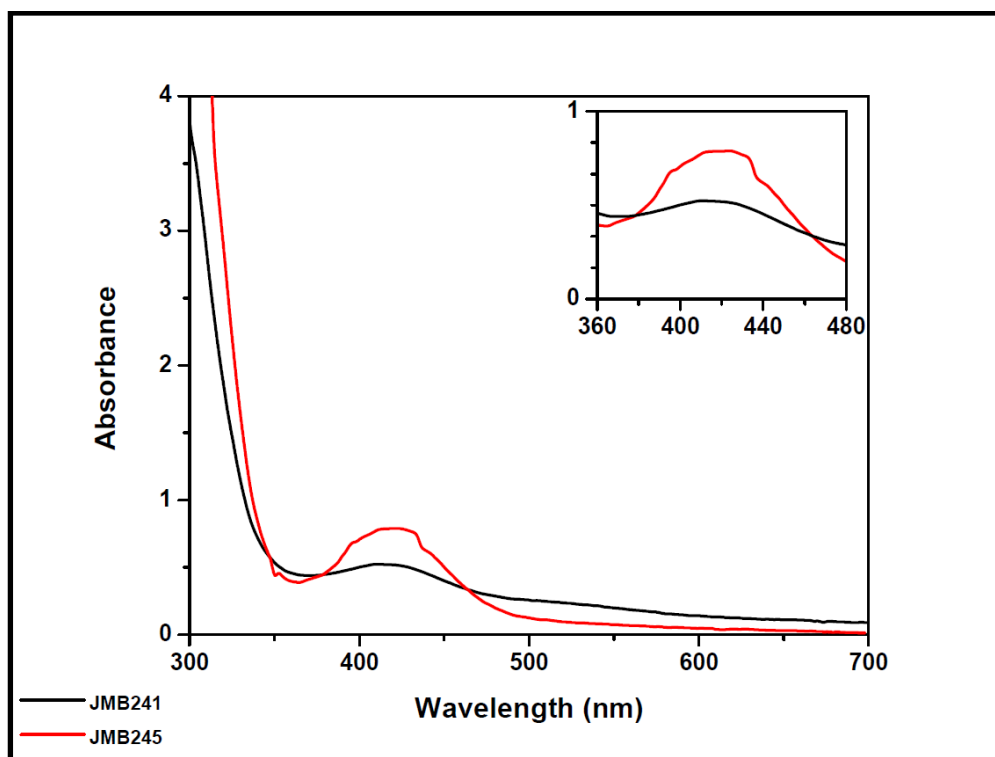
The goal of these reactions is to convert the $\text{Ni}^{\text{II}}\text{L}_2\text{X}_2$ into the $\text{Ni}^{\text{II}}\text{L}_2(\text{CH}_3)_2$, which may then be isolable or reductively elimination ethane to afford a Ni^0 species. Reactions that precipitate out Ni^0 as a nickel mirror or a black precipitate are undesired, as they suggest that the ligated Ni^0 complex is thermodynamically less stable than an unligated Ni^0 .



In a glovebox, a 20 mL scintillation vial was charged with $\text{Ni}^{\text{II}}\text{L}_2\text{Br}_2$ (20 mg, 0.045 mmol, 1.0 eq.) and THF (10 mL). To the solution was added CH_3MgCl (3.0 M in THF, 30 μL , 0.090 mmol, 2.0 eq.) and the solution became dark brown. After 6 h, the solution was filtered and concentrated. Analysis by mass spectrometry showed:

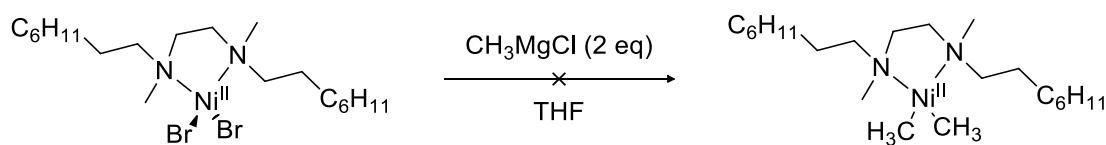
m/z	Relative Abundance (%)	Consistent Structure
225.23255	100	Ligand
297.18350	55.89	$\text{NiL}_2(\text{CH}_3)^+$
361.07850	12.89	NiL_2Br^+

UV-Vis of the reaction mixture prior to concentration:

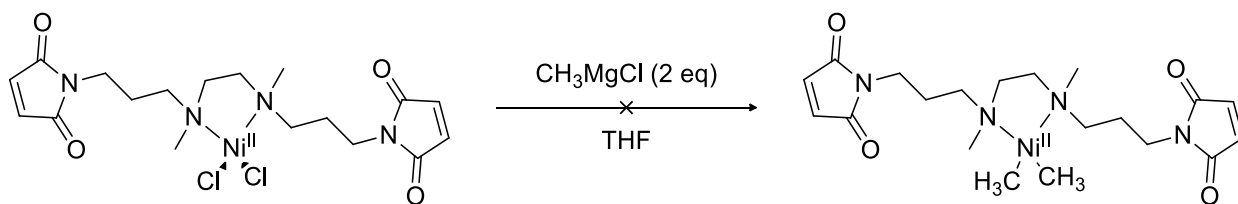


UV-Vis of JMB241 and JMB245 reaction mixtures prior to concentration

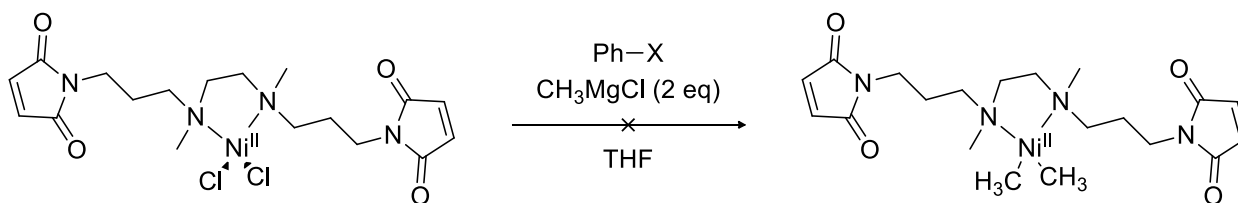
($\lambda_{\max} = 415 \text{ nm}$)



In a glovebox, a 20 mL scintillation vial was charged with $\text{Ni}^{\text{II}}\text{L}_2\text{Br}_2$ (10 mg, 0.019 mmol, 1.0 eq.) and THF (10 mL). To the purple solution was added CH_3MgCl (3.0 M in THF, 12 μL , 0.038 mmol, 2.0 eq.). The reaction became dark brown. Analysis of the reaction mixture by UV-Vis spectroscopy shown with previous reaction. This suggests one substitution is occurring.

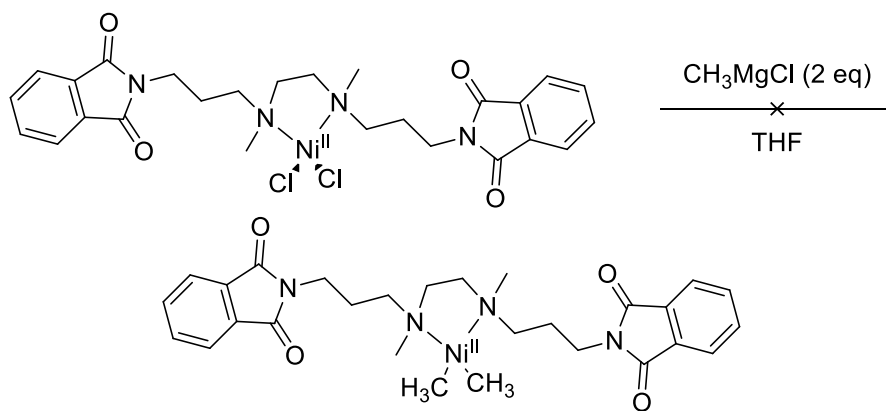


In a glovebox, a 20 mL scintillation vial was charged with $\text{Ni}^{\text{II}}\text{L}_2\text{Cl}_2$ (40 mg, 0.081 mmol, 1.0 eq.) and THF (10 mL). To the purple solution was added CH_3MgCl (3.0 M in THF, 54 μL , 0.162 mmol, 2.0 eq.) and the solution instantly became dark brown. After 2 h, the reaction was filtered into a 20 mL scintillation vial and concentrated to yield a black precipitate. The brown mixture is suggestive of one substitution occurring and the black precipitate suggests the metal complex decomposes to an unisolable product.



In a glovebox, a 20 mL scintillation vial was charged with $\text{Ni}^{\text{II}}\text{L}_2\text{Cl}_2$ (24 mg, 0.048 mmol, 1.0 eq.) and THF (15 mL). To the purple solution was added CH_3MgCl (3.0 M in THF, 33 μL , 0.098 mmol, 2.0 eq.), causing the color to change from purple to dark brown. Ten minutes later, chlorobenzene (5 mg, 5 μL , 0.048 mmol, 1.0 eq.) was added. No color change was later observed. A nickel mirror soon formed. The brown mixture is suggestive of one substitution occurring and the nickel mirror suggests the metal complex decomposes to an unisolable product.

In a glovebox, a 20 mL scintillation vial was charged with $\text{Ni}^{\text{II}}\text{L}_2\text{Cl}_2$ (15 mg, 0.030 mmol, 1.0 eq.) and THF (7 mL). To the purple solution was added CH_3MgCl (3.0 M in THF, 20 μL , 0.061 mmol, 2.0 eq.), causing the color to change from purple to dark brown. Ten minutes later, iodobenzene (6 mg, 4 μL , 0.030 mmol, 1.0 eq.) was added. No color change was later observed. A nickel mirror soon formed. The brown mixture is suggestive of one substitution occurring and the nickel mirror suggests the metal complex decomposes to an unisolable product.

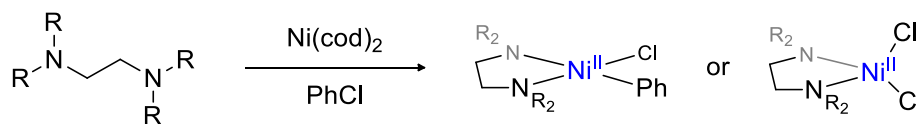


JMB261

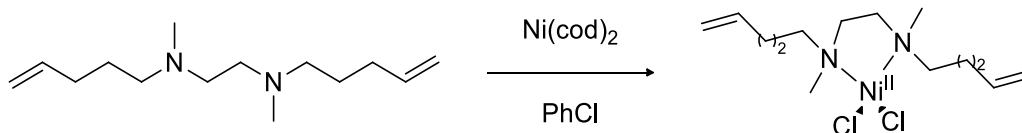
In a glovebox, a 20 mL scintillation vial was charged with $\text{Ni}^{\text{II}}\text{L}_2\text{Cl}_2$ (25 mg, 0.042 mmol, 1.0 eq.) and THF (10 mL). To the purple solution was added CH_3MgCl (3M in THF, 28 μL , 0.084 mmol, 2.0 eq.), causing the color to change from purple to dark brown. The brown mixture is suggestive of one substitution occurring.

General Route Towards Oxidative Addition Adducts of 1,2-Diamine:

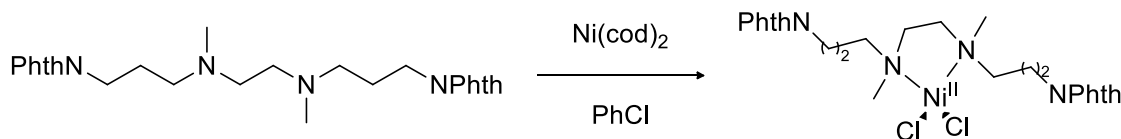
Reference: Marshall, W. J.; Grushin, V. V. *Can. J. Chem.*, **2005**, 83, 640.



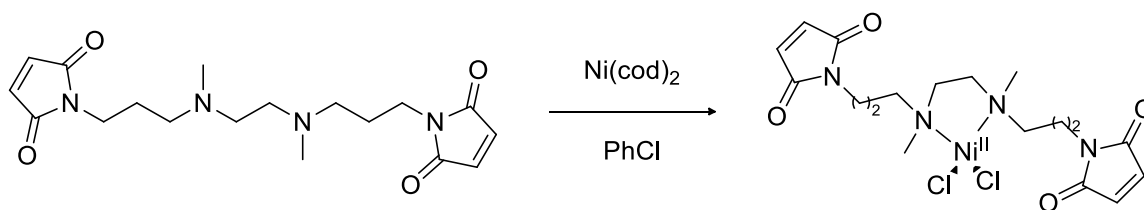
In a glovebox, a 20 mL scintillation vial was charged with Ni(cod)₂ (0.42 g, 1.52 mmol, 1.0 eq). To this vial was added a solution of the diamine (1.23 mmol) in chlorobenzene (2 mL). The mixture was allowed to stir for 6 hours at room temperature. Pentane (10 mL) was then added to the mixture and the solid was isolated by gravity filtration.



In a glovebox, a 20 mL scintillation vial was charged with Ni(cod)₂ (0.42 g, 1.52 mmol, 1.0 eq.). To this vial was added a solution of the diamine (421 mg, 1.88 mmol, 1.23 eq.) in chlorobenzene (2 mL). Instantly, a purple mixture resulted. The reaction stirred overnight. Analysis of the reaction mixture by UV-Vis spectroscopy was consistent with that observed for the Ni^{II} dihalide complexes previously synthesized, indicating the desired product had not formed. As a result, the purple solid was not isolated.



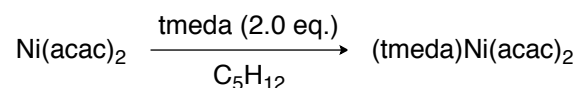
In a glovebox, a 20 mL scintillation vial was charged with Ni(cod)₂ (0.42 g, 1.52 mmol, 1.0 eq.). To this vial was added a solution of the diamine (870 mg, 1.88 mmol, 1.23 eq.) in chlorobenzene (2 mL). Instantly, a purple mixture resulted. Analysis of the reaction by UV-Vis spectroscopy was consistent with the Ni^{II} dihalide complex previously synthesized, indicating the desired product had not formed. As a result, the purple solid was not isolated.



In a glovebox, a 20 mL scintillation vial was charged with Ni(cod)₂ (0.42 g, 1.52 mmol, 1.0 eq.). To this vial was added a solution of the diamine (680 mg, 1.88 mmol, 1.23 eq.) in chlorobenzene (2 mL). Instantly, a purple mixture resulted. The reaction stirred for 3 hours and became a deep purple. Analysis of the reaction by UV-Vis spectroscopy was consistent with the Ni^{II} dihalide complex previously synthesized, indicating the desired product had not formed. As a result, the purple solid was not isolated.

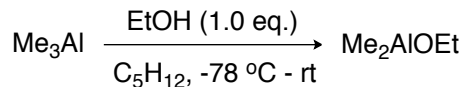
Generation of and Reactivity of (tmeda)Ni(CH₃)₂:

Reference: *J. Organomet. Chem.*, **1988**, 355, 525.



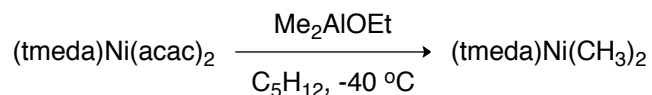
In the glovebox, a 250 mL round bottom flask was charged with anhydrous Ni(acac)₂ (25.69 g, 100 mmol, 1.0 eq.) and pentane (200 mL). To this suspension was added in one portion tmeda (30.0 mL, 23.3 g, 200 mmol, 2.0 eq.) and the reaction instantly became deep blue. The reaction stirred at room temperature for 1 h and was then filtered into another 250 mL round bottom flask, which was subsequently cooled to -40 ° overnight. Deep blue crystals formed and were isolated (30.0 g, 81%).

Reference: *J. Organomet. Chem.*, **1985**, 293, 125.

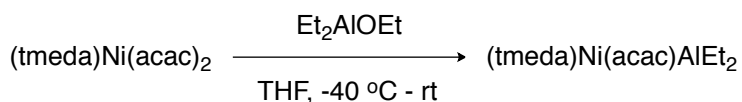


In the glovebox, a 250 mL Schlenk flask was charged with trimethylaluminum solution (2.0 M in PhCH₃, 35 mL, 70 mmol, 1.0 eq.). The Schlenk flask was brought out of the glovebox and cooled to -78 °. In the glovebox, a solution of anhydrous ethanol (3.22 g, 70 mmol, 1.0 eq.) in pentane (30 mL) was prepared and taken up in two 20 mL syringes. The solution was added to the cooled solution and the reaction was allowed to warm to room temperature. After 1 h, the solvent was removed *in vacuo* to yield a clear, colorless liquid that did not need to be further characterized.

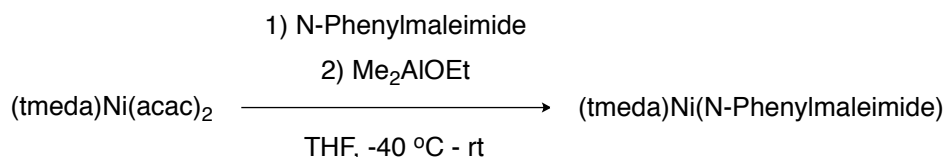
Reference: *J. Organomet. Chem.*, **1988**, 355, 525.



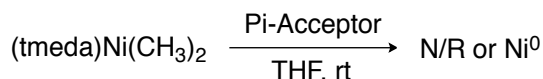
In the glovebox, a 20 mL scintillation vial was charged with (tmeda)Ni(acac)₂ (500 mg, 1.34 mmol, 1.0 eq.) and pentane (2.0 mL). The vial was cooled to -40 ° in the freezer for 30 minutes and then Me₂AlOEt (274 mg, 2.68 mmol, 2.0 eq.) was added in one portion. The reaction was allowed to warm to room temperature. After 2 h, the reaction was filtered into a 20 mL scintillation vial and cooled to -40 ° overnight. Blue-green and yellow precipitates formed, which were isolated and washed with pentane to afford a yellow solid that was dried under vacuum.



In the glovebox, a 20 mL scintillation vial was charged with (tmeda)Ni(acac)₂ (373 mg, 1.0 mmol, 1.0 eq.) and THF (10 mL). The vial was cooled to -40 °C in the freezer for 30 minutes and then Et₂AlOEt (25% w/w in PhCH₃, 1.6 mL, 2.0 mmol, 2.0 eq.) was added in one portion. The reaction was allowed to warm to room temperature and stirred overnight. The reaction was concentrated to half volume, filtered into a 20 mL scintillation vial and cooled in the freezer to afford deep red crystals. 100 mg isolated (28%). X-ray crystallographic data is at the end of this document.



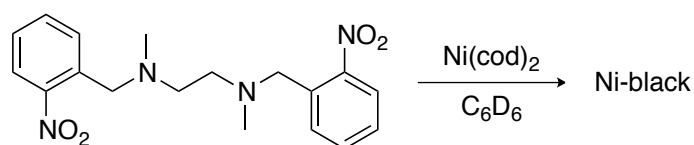
In the glovebox, a 20 mL scintillation vial was charged with (tmeda)Ni(acac)₂ (1.0 g, 2.68 mmol, 1.0 eq.), N-methylmaleimide (928 mg, 5.36 mmol, 2.0 eq.) and THF (1.0 mL). The vial was cooled to -40 °C in the freezer for 30 minutes and then Me₂AlOEt (547 mg, 5.36 mmol, 2.0 eq.) was added in one portion. The reaction was allowed to warm to room temperature. After 2 h, the reaction was filtered into a 20 mL scintillation vial and cooled in the freezer and produced deep red crystals after one week. 206 mg isolated (23%). X-ray crystallographic data is at the end of this document.



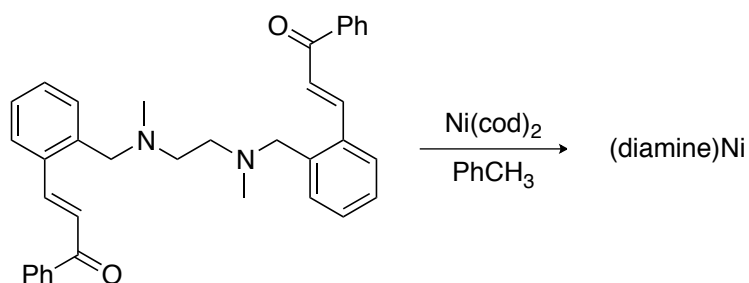
In the glovebox, a 20 mL scintillation vial was charged with (tmeda)Ni(CH₃)₂ (50 mg) and THF (10 mL). Add a small amount of the pi-acceptor and record observations.

The following pi-acceptors caused a color change from yellow to deep red: Maleic anhydride, N-methylmaleimide, N-phenylmaleimide, nitrobenzene, and methyl acrylate.

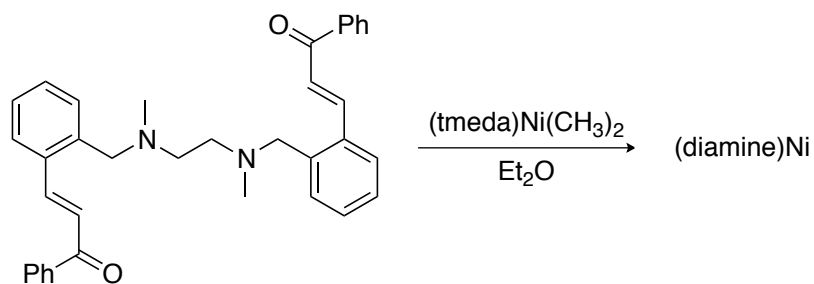
The following pi-acceptors did not cause a color change: 1,5-cyclooctadiene, benzene, and trifluorotoluene.



A 20 mL scintillation vial was charged with the ligand (50 mg, 0.277 mmol, 1.0 eq.) and deuterated benzene (3 mL). Dissolve $\text{Ni}(\text{cod})_2$ (76 mg, 0.277 mmol, 1.0 eq.) in deuterated benzene (2 mL) and add to the first solution. Follow the reaction by ^1H NMR spectroscopy. Analysis shows the presence of free ligand and cod.



A 100 mL Schlenk flask in the glovebox was charged with $\text{Ni}(\text{cod})_2$ (390 mg, 1.42 mmol, 1.0 eq.) and toluene (10 mL). Add the ligand (750 mg, 1.42 mmol, 1.0 eq.) in toluene (10 mL) and stir the reaction at room temperature. After 1 d, concentrate the reaction to half its original volume and then add pentane (25 mL). Filter the reaction to isolate a dark red solid, which is washed with pentane and dried under vacuum. Isolated 610 mg. Product remains to be fully characterized.



A 20 mL scintillation vial was charged with $(tmeda)Ni(CH_3)_2$ (36 mg, 0.176 mmol, 1.0 eq.) and Et_2O (8 mL). The vial was cooled to $-40\text{ }^\circ\text{C}$ in the freezer for 30 minutes and then a solution of the ligand (93 mg, 0.176 mmol, 1.0 eq.) in Et_2O (2 mL) was added. The reaction was allowed to warm to room temperature. After about 1 h, the reaction had become deep red. The reaction was filtered to afford a deep red solid that was dried under vacuum. Isolated 30 mg. ^1H NMR of the product shows identical spectra with the previous reaction.

Crystallographic Information for 3

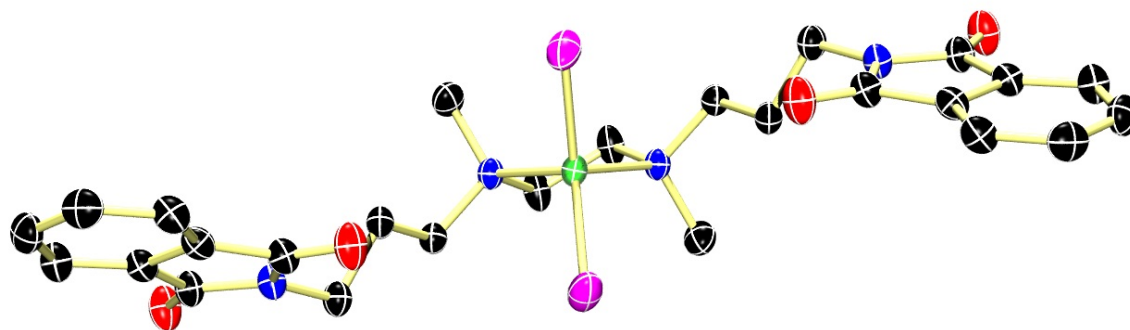


Table 2. Crystal data and structure refinement for TW4JB.

Identification code	tw4jb	
Empirical formula	$C_{30}H_{36}Cl_2N_6NiO_4$	
Formula weight	674.26	
Temperature	173 K	
Wavelength	0.71073 Å	
Crystal system	Monoclinic	
Space group	$C2/c$	
Unit cell dimensions	$a = 30.094(3)\text{ \AA}$	$a = 90^\circ$.

	$b = 7.6593(7) \text{ \AA}$	$b = 107.523(2)^\circ$.
	$c = 14.5674(13) \text{ \AA}$	$g = 90^\circ$.
Volume	$3202.0(5) \text{ \AA}^3$	
Z	4	
Density (calculated)	1.399 Mg/m^3	
Absorption coefficient	0.812 mm^{-1}	
F(000)	1408	
Crystal size	$0.430 \times 0.200 \times 0.096 \text{ mm}^3$	
Theta range for data collection	$1.42 \text{ to } 27.48^\circ$.	
Index ranges	$-38 \leq h \leq 38, -9 \leq k \leq 9, -18 \leq l \leq 18$	
Reflections collected	7051	
Independent reflections	3661 [R(int) = 0.0442]	
Completeness to theta = 27.48°	99.7 %	
Absorption correction	Semi-empirical from equivalents	
Max. and min. transmission	0.745908 and 0.603938	
Refinement method	Full-matrix least-squares on F^2	
Data / restraints / parameters	3661 / 0 / 267	
Goodness-of-fit on F^2	1.042	
Final R indices [I > 2sigma(I)]	R1 = 0.0482, wR2 = 0.1072	
R indices (all data)	R1 = 0.0704, wR2 = 0.1177	
Largest diff. peak and hole	0.483 and $-0.289 \text{ e.\AA}^{-3}$	

Table 3. Atomic coordinates ($\times 10^4$) and equivalent isotropic displacement parameters ($\text{\AA}^2 \times 10^3$) for TW4JB. $U(\text{eq})$ is defined as one third of the trace of the orthogonalized U^{ij} tensor.

	x	y	z	$U(\text{eq})$
Ni(1)	0	10666(1)	2500	26(1)
Cl(1)	-584(1)	9428(1)	1379(1)	51(1)
O(1)	1841(1)	10326(3)	263(2)	45(1)
O(2)	952(1)	6433(3)	1305(2)	46(1)
N(1)	261(1)	12577(3)	1825(2)	28(1)
C(3)	809(1)	10622(4)	1322(2)	30(1)
N(2)	1381(1)	8679(3)	949(2)	31(1)
C(2)	759(1)	12221(4)	1905(2)	30(1)
C(5)	1643(1)	8982(4)	318(2)	33(1)
C(4)	1309(1)	9976(4)	1624(2)	33(1)
C(9)	1241(1)	4531(4)	-344(2)	37(1)
C(8)	1190(1)	7020(4)	839(2)	33(1)
C(6)	1619(1)	7331(3)	-233(2)	32(1)
C(12)	1822(1)	6905(4)	-940(2)	38(1)
C(1)	229(1)	14179(4)	2383(2)	37(1)
C(7)	1339(1)	6172(3)	63(2)	32(1)
C(13)	-7(1)	12846(5)	800(2)	40(1)
C(11)	1720(1)	5256(4)	-1358(2)	41(1)
C(10)	1433(1)	4103(4)	-1074(2)	43(1)
N(3)	2390(1)	7495(4)	2185(2)	62(1)
C(14)	2454(1)	8037(4)	2936(2)	38(1)
C(15)	2536(1)	8726(5)	3898(2)	43(1)

Table 4. Bond lengths [\AA] and angles [$^\circ$] for TW4JB.

Ni(1)-Cl(1)#1	2.2194(8)
Ni(1)-Cl(1)	2.2194(8)
Ni(1)-N(1)#1	2.048(2)
Ni(1)-N(1)	2.047(2)
O(1)-C(5)	1.203(3)
O(2)-C(8)	1.210(3)
N(1)-C(2)	1.494(3)
N(1)-C(1)	1.491(3)
N(1)-C(13)	1.483(4)
C(3)-C(2)	1.523(4)
C(3)-C(4)	1.519(4)
C(3)-H(3A)	0.95(3)
C(3)-H(3B)	0.96(3)
N(2)-C(5)	1.398(3)
N(2)-C(4)	1.460(3)
N(2)-C(8)	1.385(3)
C(2)-H(2A)	0.93(3)
C(2)-H(2B)	1.01(3)
C(5)-C(6)	1.488(4)
C(4)-H(4A)	0.95(3)
C(4)-H(4B)	0.93(3)
C(9)-C(7)	1.383(4)
C(9)-C(10)	1.393(4)
C(9)-H(9)	0.93(3)
C(8)-C(7)	1.486(4)
C(6)-C(12)	1.385(4)
C(6)-C(7)	1.380(4)
C(12)-C(11)	1.395(4)
C(12)-H(12)	0.89(3)
C(1)-C(1)#1	1.519(5)
C(1)-H(1A)	1.03(4)
C(1)-H(1B)	0.90(3)
C(13)-H(13A)	0.92(3)
C(13)-H(13B)	0.90(5)

C(13)-H(13C)	0.96(3)
C(11)-C(10)	1.383(5)
C(11)-H(11)	0.87(3)
C(10)-H(10)	0.90(4)
N(3)-C(14)	1.130(4)
C(14)-C(15)	1.448(4)
C(15)-H(15A)	0.96(4)
C(15)-H(15B)	0.87(4)
C(15)-H(15C)	0.99(4)
Cl(1)-Ni(1)-Cl(1)#1	129.41(5)
N(1)-Ni(1)-Cl(1)#1	109.00(7)
N(1)#1-Ni(1)-Cl(1)#1	106.58(6)
N(1)#1-Ni(1)-Cl(1)	109.00(7)
N(1)-Ni(1)-Cl(1)	106.58(6)
N(1)-Ni(1)-N(1)#1	88.74(12)
C(2)-N(1)-Ni(1)	110.72(16)
C(1)-N(1)-Ni(1)	103.28(15)
C(1)-N(1)-C(2)	109.6(2)
C(13)-N(1)-Ni(1)	114.34(19)
C(13)-N(1)-C(2)	109.4(2)
C(13)-N(1)-C(1)	109.3(2)
C(2)-C(3)-H(3A)	109.3(16)
C(2)-C(3)-H(3B)	109.7(17)
C(4)-C(3)-C(2)	110.8(2)
C(4)-C(3)-H(3A)	111.1(16)
C(4)-C(3)-H(3B)	109.7(17)
H(3A)-C(3)-H(3B)	106(2)
C(5)-N(2)-C(4)	123.9(2)
C(8)-N(2)-C(5)	112.0(2)
C(8)-N(2)-C(4)	124.1(2)
N(1)-C(2)-C(3)	111.5(2)
N(1)-C(2)-H(2A)	107.9(15)
N(1)-C(2)-H(2B)	107.6(14)
C(3)-C(2)-H(2A)	110.1(16)
C(3)-C(2)-H(2B)	111.9(14)

H(2A)-C(2)-H(2B)	108(2)
O(1)-C(5)-N(2)	125.0(3)
O(1)-C(5)-C(6)	129.4(2)
N(2)-C(5)-C(6)	105.6(2)
C(3)-C(4)-H(4A)	109.2(19)
C(3)-C(4)-H(4B)	110(2)
N(2)-C(4)-C(3)	111.2(2)
N(2)-C(4)-H(4A)	107.0(18)
N(2)-C(4)-H(4B)	109.8(19)
H(4A)-C(4)-H(4B)	110(3)
C(7)-C(9)-C(10)	117.2(3)
C(7)-C(9)-H(9)	120.4(17)
C(10)-C(9)-H(9)	122.3(17)
O(2)-C(8)-N(2)	124.9(3)
O(2)-C(8)-C(7)	129.0(3)
N(2)-C(8)-C(7)	106.1(2)
C(12)-C(6)-C(5)	129.9(2)
C(7)-C(6)-C(5)	108.2(2)
C(7)-C(6)-C(12)	121.9(3)
C(6)-C(12)-C(11)	116.7(3)
C(6)-C(12)-H(12)	122.1(19)
C(11)-C(12)-H(12)	121.1(19)
N(1)-C(1)-C(1)#1	109.5(2)
N(1)-C(1)-H(1A)	109.1(19)
N(1)-C(1)-H(1B)	111.0(19)
C(1)#1-C(1)-H(1A)	106.8(19)
C(1)#1-C(1)-H(1B)	114(2)
H(1A)-C(1)-H(1B)	106(3)
C(9)-C(7)-C(8)	130.4(3)
C(6)-C(7)-C(9)	121.5(3)
C(6)-C(7)-C(8)	108.1(2)
N(1)-C(13)-H(13A)	113.5(19)
N(1)-C(13)-H(13B)	108(3)
N(1)-C(13)-H(13C)	111.2(19)
H(13A)-C(13)-H(13B)	110(3)
H(13A)-C(13)-H(13C)	107(3)

H(13B)-C(13)-H(13C)	106(3)
C(12)-C(11)-H(11)	117(2)
C(10)-C(11)-C(12)	121.5(3)
C(10)-C(11)-H(11)	121(2)
C(9)-C(10)-H(10)	116(2)
C(11)-C(10)-C(9)	121.2(3)
C(11)-C(10)-H(10)	123(2)
N(3)-C(14)-C(15)	179.8(4)
C(14)-C(15)-H(15A)	110(2)
C(14)-C(15)-H(15B)	109(3)
C(14)-C(15)-H(15C)	108(2)
H(15A)-C(15)-H(15B)	109(4)
H(15A)-C(15)-H(15C)	108(3)
H(15B)-C(15)-H(15C)	112(3)

Symmetry transformations used to generate equivalent atoms:

#1 _____

Table 5. Anisotropic displacement parameters ($\text{\AA}^2 \times 10^3$) for TW4JB. The anisotropic displacement factor exponent takes the form: $-2p^2[h^2 a^*2U^{11} + \dots + 2 h k a^* b^* U^{12}]$

	U ¹¹	U ²²	U ³³	U ²³	U ¹³	U ¹²
Ni(1)	34(1)	20(1)	26(1)	0	14(1)	0
Cl(1)	57(1)	58(1)	40(1)	-18(1)	19(1)	-26(1)
O(1)	55(1)	30(1)	60(1)	-5(1)	34(1)	-12(1)
O(2)	59(1)	32(1)	58(1)	2(1)	35(1)	-6(1)
N(1)	33(1)	24(1)	29(1)	1(1)	14(1)	-1(1)
C(3)	33(1)	30(1)	30(1)	-2(1)	14(1)	-2(1)
N(2)	34(1)	26(1)	37(1)	-4(1)	18(1)	-3(1)
C(2)	32(1)	29(1)	30(1)	-1(1)	12(1)	-2(1)
C(5)	37(2)	29(1)	39(2)	-1(1)	18(1)	1(1)
C(4)	38(2)	31(1)	35(2)	-3(1)	16(1)	-1(1)
C(9)	37(2)	28(1)	49(2)	-4(1)	16(1)	-3(1)
C(8)	35(1)	26(1)	40(2)	2(1)	16(1)	-1(1)
C(6)	32(1)	28(1)	37(1)	1(1)	12(1)	1(1)
C(12)	42(2)	34(2)	44(2)	0(1)	22(1)	0(1)
C(1)	47(2)	21(1)	52(2)	-3(1)	31(2)	-4(1)
C(7)	30(1)	26(1)	39(1)	2(1)	11(1)	3(1)
C(13)	43(2)	42(2)	35(2)	11(1)	14(1)	5(1)
C(11)	47(2)	39(2)	42(2)	-5(1)	21(1)	8(1)
C(10)	49(2)	30(2)	49(2)	-9(1)	12(1)	4(1)
N(3)	75(2)	64(2)	50(2)	-10(2)	22(2)	-1(2)
C(14)	40(2)	34(2)	43(2)	5(1)	18(1)	4(1)
C(15)	52(2)	42(2)	37(2)	4(1)	13(2)	9(2)

Table 6. Hydrogen coordinates ($\times 10^4$) and isotropic displacement parameters ($\text{\AA}^2 \times 10^3$) for TW4JB.

	x	y	z	U(eq)
H(1A)	491(13)	14160(40)	3030(30)	49(9)
H(3A)	705(9)	10900(30)	650(20)	22(6)
H(2A)	920(9)	12050(30)	2553(19)	20(6)
H(9)	1041(10)	3790(40)	-157(18)	23(7)
H(2B)	890(9)	13310(40)	1686(17)	19(6)
H(13A)	-32(10)	11860(50)	430(20)	34(8)
H(4A)	1511(11)	10930(40)	1620(20)	35(8)
H(3B)	607(10)	9710(40)	1410(20)	31(7)
H(1B)	276(11)	15150(40)	2070(20)	35(8)
H(15A)	2676(14)	9870(60)	3940(30)	69(12)
H(10)	1367(11)	3030(50)	-1330(20)	46(9)
H(12)	2019(10)	7620(40)	-1100(20)	33(8)
H(4B)	1385(11)	9500(40)	2240(20)	40(9)
H(13B)	130(15)	13700(60)	560(30)	70(12)
H(13C)	-318(12)	13240(40)	730(20)	47(9)
H(11)	1832(11)	5000(40)	-1830(20)	42(9)
H(15B)	2272(15)	8810(50)	4020(30)	68(12)
H(15C)	2757(14)	7940(50)	4360(30)	68(11)

Table 7. Torsion angles [°] for TW4JB.

Ni(1)-N(1)-C(2)-C(3)	68.3(2)
Ni(1)-N(1)-C(1)-C(1)#1	-41.1(3)
Cl(1)-Ni(1)-N(1)-C(2)	-118.81(15)
Cl(1)#1-Ni(1)-N(1)-C(2)	24.62(17)
Cl(1)#1-Ni(1)-N(1)-C(1)	-92.64(17)
Cl(1)-Ni(1)-N(1)-C(1)	123.93(17)
Cl(1)#1-Ni(1)-N(1)-C(13)	148.74(18)
Cl(1)-Ni(1)-N(1)-C(13)	5.3(2)
O(1)-C(5)-C(6)-C(12)	0.8(5)
O(1)-C(5)-C(6)-C(7)	-178.2(3)
O(2)-C(8)-C(7)-C(9)	1.7(5)
O(2)-C(8)-C(7)-C(6)	-178.0(3)
N(1)#1-Ni(1)-N(1)-C(2)	131.73(19)
N(1)#1-Ni(1)-N(1)-C(1)	14.47(14)
N(1)#1-Ni(1)-N(1)-C(13)	-104.1(2)
N(2)-C(5)-C(6)-C(12)	-179.0(3)
N(2)-C(5)-C(6)-C(7)	2.0(3)
N(2)-C(8)-C(7)-C(9)	-178.8(3)
N(2)-C(8)-C(7)-C(6)	1.5(3)
C(2)-N(1)-C(1)-C(1)#1	-159.1(3)
C(2)-C(3)-C(4)-N(2)	-168.5(2)
C(5)-N(2)-C(4)-C(3)	109.6(3)
C(5)-N(2)-C(8)-O(2)	179.3(3)
C(5)-N(2)-C(8)-C(7)	-0.2(3)
C(5)-C(6)-C(12)-C(11)	-177.4(3)
C(5)-C(6)-C(7)-C(9)	178.2(3)
C(5)-C(6)-C(7)-C(8)	-2.1(3)
C(4)-C(3)-C(2)-N(1)	-164.0(2)
C(4)-N(2)-C(5)-O(1)	0.6(5)
C(4)-N(2)-C(5)-C(6)	-179.5(2)
C(4)-N(2)-C(8)-O(2)	-2.2(4)
C(4)-N(2)-C(8)-C(7)	178.2(2)
C(8)-N(2)-C(5)-O(1)	179.1(3)
C(8)-N(2)-C(5)-C(6)	-1.0(3)

C(8)-N(2)-C(4)-C(3)	-68.7(3)
C(6)-C(12)-C(11)-C(10)	-0.4(5)
C(12)-C(6)-C(7)-C(9)	-1.0(4)
C(12)-C(6)-C(7)-C(8)	178.8(3)
C(12)-C(11)-C(10)-C(9)	-1.3(5)
C(1)-N(1)-C(2)-C(3)	-178.4(2)
C(7)-C(9)-C(10)-C(11)	1.9(5)
C(7)-C(6)-C(12)-C(11)	1.5(4)
C(13)-N(1)-C(2)-C(3)	-58.6(3)
C(13)-N(1)-C(1)-C(1)#1	81.0(3)
C(10)-C(9)-C(7)-C(8)	179.6(3)
C(10)-C(9)-C(7)-C(6)	-0.7(4)

Symmetry transformations used to generate equivalent atoms:

#1 _____

Crystallographic Information for 4

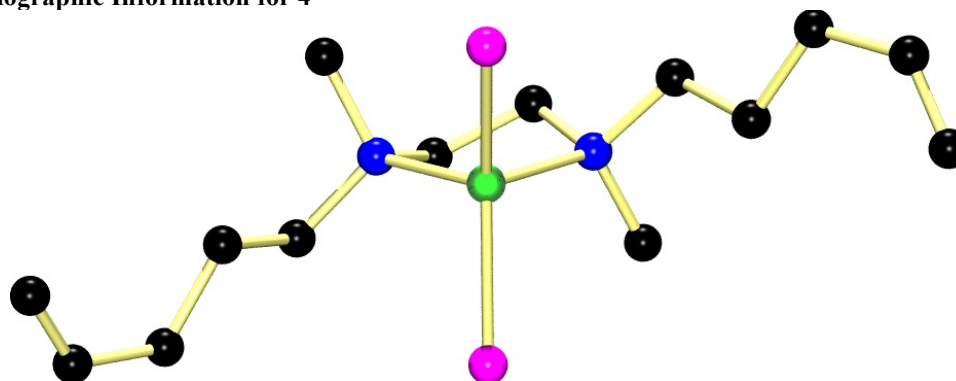


Table 1. Crystal data and structure refinement for JMB228BM_FIN.

Identification code	jmb228bm	
Empirical formula	C ₁₄ H ₂₈ Br ₂ N ₂ Ni	
Formula weight	442.91	
Temperature	173 K	
Wavelength	0.71073 Å	
Crystal system	Orthorhombic	
Space group	P b c n	
Unit cell dimensions	a = 7.9488(14) Å	a = 90°.
	b = 12.123(2) Å	b = 90°.
	c = 18.638(3) Å	g = 90°.

Volume	1796.0(6) Å ³
Z	4
Density (calculated)	1.638 Mg/m ³
Absorption coefficient	5.521 mm ⁻¹
F(000)	896
Crystal size	0.334 x 0.274 x 0.211 mm ³
Theta range for data collection	2.19 to 27.48°.
Index ranges	-10<=h<=9, -15<=k<=14, -24<=l<=24
Reflections collected	15831
Independent reflections	2064 [R(int) = 0.0640]
Completeness to theta = 27.48°	100.0 %
Absorption correction	Semi-empirical from equivalents
Max. and min. transmission	0.2175 and 0.1266
Refinement method	Full-matrix least-squares on F ²
Data / restraints / parameters	2064 / 7 / 98
Goodness-of-fit on F ²	1.108
Final R indices [I>2sigma(I)]	R1 = 0.0458, wR2 = 0.1036
R indices (all data)	R1 = 0.0632, wR2 = 0.1097
Largest diff. peak and hole	1.074 and -0.395 e.Å ⁻³

Table 2. Atomic coordinates ($\times 10^4$) and equivalent isotropic displacement parameters ($\text{\AA}^2 \times 10^3$) for JMB228BM_FIN. $U(\text{eq})$ is defined as one third of the trace of the orthogonalized U^{ij} tensor.

	x	y	z	$U(\text{eq})$
Br(1)	3275(2)	6183(2)	1653(1)	38(1)
Ni(1)	5000	5278(1)	2500	28(1)
Br(1')	2732(19)	5827(13)	1757(6)	52(2)
N(1)	6340(4)	4077(3)	1988(2)	26(1)
C(1)	9706(7)	6757(5)	112(3)	48(2)
C(2)	8384(7)	6325(4)	-159(3)	43(2)
C(3)	7237(6)	5491(4)	188(2)	34(1)
C(4)	7569(6)	5217(4)	972(2)	30(1)
C(5)	6476(6)	4255(4)	1190(2)	31(1)
C(6)	8057(6)	3926(4)	2285(3)	39(2)
C(7)	5340(6)	3070(3)	2120(2)	29(1)

Table 3. Bond lengths [Å] and angles [°] for JMB228BM_FIN.

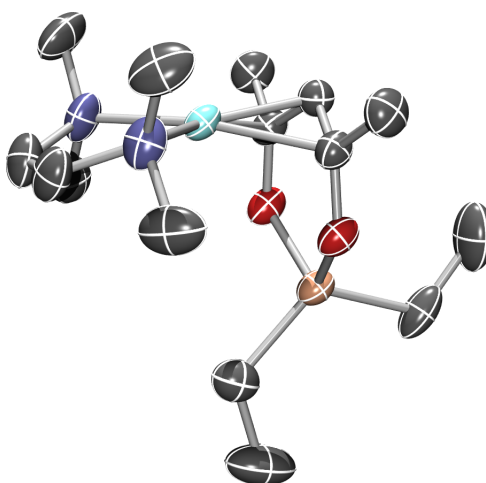
Br(1)-Ni(1)	2.3616(15)
Br(1')-Ni(1)	2.369(14)
Ni(1)-N(1)	2.041(4)
Ni(1)-N(1)#1	2.041(4)
N(1)-C(5)	1.507(5)
N(1)-C(6)	1.484(6)
N(1)-C(7)	1.477(5)
C(1)-C(2)	1.278(8)
C(2)-C(3)	1.507(7)
C(3)-C(4)	1.522(5)
C(4)-C(5)	1.510(7)
C(7)-C(7)#1	1.516(5)
C(1)-H(1A)	0.9500
C(1)-H(1B)	0.9500
C(2)-H(2)	0.9500
C(3)-H(3A)	0.9900
C(3)-H(3B)	0.9900
C(4)-H(4A)	0.9900
C(4)-H(4B)	0.9900
C(5)-H(5A)	0.9900
C(5)-H(5B)	0.9900
C(6)-H(6A)	0.9800
C(6)-H(6B)	0.9800
C(6)-H(6C)	0.9800
C(7)-H(7A)	0.9900
C(7)-H(7B)	0.9900
Br(1)-Ni(1)-N(1)	108.79(11)
Br(1)-Ni(1)-Br(1)#1	124.59(7)
Br(1)-Ni(1)-N(1)#1	109.95(10)
Br(1')-Ni(1)-N(1)	108.9(3)
Br(1')-Ni(1)-Br(1')#1	147.4(5)
Br(1')-Ni(1)-N(1)#1	94.4(4)
Br(1)#1-Ni(1)-N(1)	109.95(10)

Br(1')#1-Ni(1)-N(1)	94.4(4)
N(1)-Ni(1)-N(1)#1	88.99(14)
Br(1)#1-Ni(1)-N(1)#1	108.79(11)
Br(1')#1-Ni(1)-N(1)#1	108.9(3)
Ni(1)-N(1)-C(5)	113.4(3)
Ni(1)-N(1)-C(6)	113.2(3)
Ni(1)-N(1)-C(7)	103.3(2)
C(5)-N(1)-C(6)	108.7(3)
C(5)-N(1)-C(7)	108.7(3)
C(6)-N(1)-C(7)	109.3(3)
C(1)-C(2)-C(3)	127.1(5)
C(2)-C(3)-C(4)	117.0(4)
C(3)-C(4)-C(5)	109.1(4)
N(1)-C(5)-C(4)	114.7(3)
N(1)-C(7)-C(7)#1	110.3(3)
C(2)-C(1)-H(1A)	120.00
C(2)-C(1)-H(1B)	120.00
H(1A)-C(1)-H(1B)	120.00
C(1)-C(2)-H(2)	117.00
C(3)-C(2)-H(2)	116.00
C(2)-C(3)-H(3A)	108.00
C(2)-C(3)-H(3B)	108.00
C(4)-C(3)-H(3A)	108.00
C(4)-C(3)-H(3B)	108.00
H(3A)-C(3)-H(3B)	107.00
C(3)-C(4)-H(4A)	110.00
C(3)-C(4)-H(4B)	110.00
C(5)-C(4)-H(4A)	110.00
C(5)-C(4)-H(4B)	110.00
H(4A)-C(4)-H(4B)	108.00
N(1)-C(5)-H(5A)	109.00
N(1)-C(5)-H(5B)	109.00
C(4)-C(5)-H(5A)	109.00
C(4)-C(5)-H(5B)	109.00
H(5A)-C(5)-H(5B)	108.00
N(1)-C(6)-H(6A)	109.00

N(1)-C(6)-H(6B)	109.00
N(1)-C(6)-H(6C)	109.00
H(6A)-C(6)-H(6B)	109.00
H(6A)-C(6)-H(6C)	109.00
H(6B)-C(6)-H(6C)	110.00
N(1)-C(7)-H(7A)	110.00
N(1)-C(7)-H(7B)	110.00
H(7A)-C(7)-H(7B)	108.00
C(7)#1-C(7)-H(7A)	110.00
C(7)#1-C(7)-H(7B)	110.00

Symmetry transformations used to generate equivalent atoms:

#1 $1/2-x+1, 1/2-y, 1/2+z$



Identification code	jmb315d	
Empirical formula	C ₁₅ H ₃₃ Al N ₂ Ni O ₂	
Formula weight	359.12	
Temperature	446(2) K	
Wavelength	0.71073 Å	
Crystal system	Orthorhombic	
Space group	P n m a	
Unit cell dimensions	a = 14.363(4) Å	α = 90°.
	b = 12.260(3) Å	β = 90°.
	c = 10.795(3) Å	γ = 90°.
Volume	1900.9(8) Å ³	

Z	4
Density (calculated)	1.255 Mg/m ³
Absorption coefficient	1.072 mm ⁻¹
F(000)	776
Crystal size	0.242 x 0.224 x 0.128 mm ³
Theta range for data collection	2.360 to 28.282°.
Index ranges	-19<=h<=19, -16<=k<=16, -14<=l<=14
Reflections collected	13774
Independent reflections	2455 [R(int) = 0.0520]
Completeness to theta = 25.242°	99.9 %
Refinement method	Full-matrix least-squares on F ²
Data / restraints / parameters	2455 / 7 / 125
Goodness-of-fit on F ²	1.090
Final R indices [I>2sigma(I)]	R1 = 0.0477, wR2 = 0.1253
R indices (all data)	R1 = 0.0675, wR2 = 0.1379
Extinction coefficient	n/a
Largest diff. peak and hole	0.644 and -0.449 e.Å ⁻³

Table 2. Atomic coordinates ($\times 10^4$) and equivalent isotropic displacement parameters ($\text{\AA}^2 \times 10^3$) for jmb315d. $U(\text{eq})$ is defined as one third of the trace of the orthogonalized U^{ij} tensor.

	x	y	z	$U(\text{eq})$
C(1)	1633(1)	691(1)	-246(1)	68(1)
C(2)	2802(1)	619(1)	1302(1)	72(1)
C(3A)	2661(1)	1963(1)	-515(1)	56(1)
C(4)	489(1)	2500	2708(1)	36(1)
C(4A)	3026(1)	3010(1)	22(1)	56(1)
C(5)	942(1)	3506(1)	2919(1)	36(1)
C(6)	439(1)	4556(1)	2633(1)	50(1)
C(7)	1496(1)	2500	6271(1)	59(1)
C(8)	438(1)	2500	6208(2)	89(1)
C(9)	3457(1)	2500	4521(2)	56(1)
C(10)	4010(1)	2500	5719(2)	87(1)
N(1)	2249(1)	1381(1)	522(1)	48(1)
O(1)	1631(1)	3630(1)	3752(1)	39(1)
Al(1)	2085(1)	2500	4617(1)	37(1)
Ni(1)	1540(1)	2500	1535(1)	33(1)

Table 3. Bond lengths [\AA] and angles [$^\circ$] for jmb315d.

C(1)-N(1)	1.4785(12)
C(1)-H(1A)	0.835(13)
C(1)-H(1B)	0.967(13)
C(1)-H(1C)	0.900(13)
C(2)-N(1)	1.4867(13)
C(2)-H(2A)	0.9600
C(2)-H(2B)	0.9600
C(2)-H(2C)	0.9600
C(3A)-N(1)	1.4539(9)
C(3A)-C(4A)	1.5036(12)
C(3A)-H(3AA)	0.9700
C(3A)-H(3AB)	0.9700
C(4)-C(5)	1.4125(9)
C(4)-Ni(1)	1.9693(11)
C(4)-H(4)	0.988(2)
C(4A)-N(1)#1	1.4466(9)
C(4A)-H(4AA)	0.9700
C(4A)-H(4AB)	0.9700
C(5)-O(1)	1.3454(10)
C(5)-C(6)	1.5092(12)
C(5)-Ni(1)	2.1182(8)
C(6)-H(6A)	0.9600
C(6)-H(6B)	0.9600
C(6)-H(6C)	0.9600
C(7)-C(8)	1.522(2)
C(7)-Al(1)	1.9750(14)
C(7)-H(7B)	0.9700
C(7)-H(7A)	0.9700
C(8)-H(8C)	0.9611
C(8)-H(8B)	0.9611
C(8)-H(8A)	0.9611
C(9)-C(10)	1.518(2)
C(9)-Al(1)	1.9737(14)
C(9)-H(9A)	0.9700

C(9)-H(9B)	0.9700
C(10)-H(10C)	0.9600
C(10)-H(10A)	0.9600
C(10)-H(10B)	0.9600
N(1)-C(4A)#1	1.4466(9)
N(1)-Ni(1)	2.0293(6)
O(1)-Al(1)	1.7939(7)
Ni(1)-C(4)#1	1.9693(11)
Ni(1)-C(5)#1	2.1182(8)
N(1)-C(1)-H(1A)	109.7(9)
N(1)-C(1)-H(1B)	111.2(8)
H(1A)-C(1)-H(1B)	114.0(12)
N(1)-C(1)-H(1C)	107.8(8)
H(1A)-C(1)-H(1C)	109.4(12)
H(1B)-C(1)-H(1C)	104.4(11)
N(1)-C(3A)-C(4A)	105.30(6)
C(5)#1-C(4)-C(5)	121.56(9)
C(5)-C(4)-Ni(1)	75.57(5)
C(5)-C(4)-H(4)	118.44(5)
Ni(1)-C(4)-H(4)	108.01(17)
N(1)#1-C(4A)-C(3A)	108.41(6)
O(1)-C(5)-C(4)#1	123.05(7)
O(1)-C(5)-C(6)	113.08(7)
C(4)-C(5)-C(6)	119.43(7)
O(1)-C(5)-Ni(1)	103.86(5)
C(4)#1-C(5)-Ni(1)	64.20(5)
C(6)-C(5)-Ni(1)	123.14(6)
C(8)-C(7)-Al(1)	112.82(10)
C(10)-C(9)-Al(1)	118.50(11)
C(3A)-N(1)-C(1)	95.32(6)
C(4A)#1-N(1)-C(2)	97.09(7)
C(3A)-N(1)-C(2)	121.83(7)
C(1)-N(1)-C(2)	106.12(7)
C(1)-N(1)-Ni(1)	112.86(6)
C(2)-N(1)-Ni(1)	112.82(5)

C(5)-O(1)-Al(1)	121.88(5)
O(1)#1-Al(1)-O(1)	101.10(4)
O(1)-Al(1)-C(9)	109.62(3)
O(1)-Al(1)-C(7)	108.35(4)
C(9)-Al(1)-C(7)	118.40(7)
C(4)#1-Ni(1)-N(1)	136.981(18)
N(1)-Ni(1)-N(1)#1	85.10(3)
N(1)-Ni(1)-C(5)#1	100.95(3)
N(1)#1-Ni(1)-C(5)#1	167.70(3)
C(4)-Ni(1)-C(5)	40.23(3)
N(1)-Ni(1)-C(5)	167.70(3)
N(1)#1-Ni(1)-C(5)	100.95(3)
C(5)#1-Ni(1)-C(5)	71.18(5)

Symmetry transformations used to generate equivalent atoms:

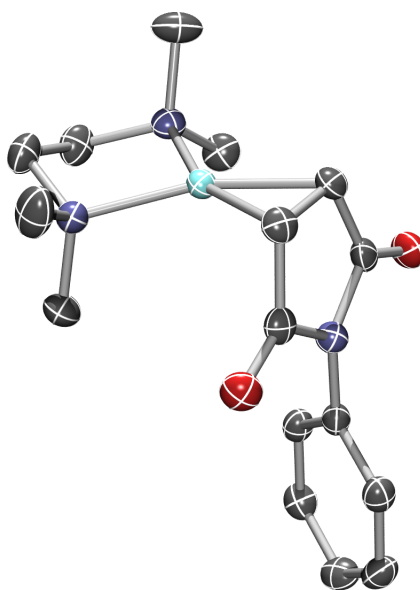
#1 $x, -y+1/2, z$

Table 4. Anisotropic displacement parameters ($\text{\AA}^2 \times 10^3$) for jmb315d. The anisotropic displacement factor exponent takes the form: $-2\pi^2 [h^2 a^{*2} U^{11} + \dots + 2 h k a^* b^* U^{12}]$

	U^{11}	U^{22}	U^{33}	U^{23}	U^{13}	U^{12}
C(1)	100(1)	59(1)	45(1)	-23(1)	-13(1)	16(1)
C(2)	74(1)	78(1)	64(1)	-26(1)	-11(1)	32(1)
C(3A)	72(1)	60(1)	35(1)	0(1)	14(1)	3(1)
C(4)	38(1)	35(1)	35(1)	0	0(1)	0
C(4A)	72(1)	60(1)	35(1)	0(1)	14(1)	3(1)
C(5)	44(1)	32(1)	32(1)	0(1)	-1(1)	3(1)
C(6)	58(1)	35(1)	55(1)	1(1)	0(1)	9(1)
C(7)	102(1)	44(1)	30(1)	0	4(1)	0
C(8)	100(1)	86(1)	80(1)	0	50(1)	0
C(9)	53(1)	50(1)	65(1)	0	-9(1)	0
C(10)	76(1)	74(1)	110(1)	0	-46(1)	0
N(1)	67(1)	37(1)	40(1)	-9(1)	9(1)	0(1)
O(1)	54(1)	29(1)	32(1)	-1(1)	-4(1)	-2(1)
Al(1)	46(1)	37(1)	28(1)	0	-5(1)	0
Ni(1)	45(1)	29(1)	25(1)	0	-3(1)	0

Table 5. Hydrogen coordinates ($\times 10^4$) and isotropic displacement parameters ($\text{\AA}^2 \times 10^{-3}$) for jmb315d.

	x	y	z	U(eq)
H(1A)	1270(9)	342(10)	209(12)	102
H(1B)	1989(9)	240(11)	-807(12)	102
H(1C)	1303(9)	1133(11)	-744(12)	102
H(2A)	3236	1027	1794	108
H(2B)	3135	120	779	108
H(2C)	2391	218	1836	108
H(3AA)	2197	2109	-1147	67
H(3AB)	3162	1542	-880	67
H(4AA)	3473	2855	672	67
H(4AB)	3335	3434	-615	67
H(6A)	882	5103	2392	74
H(6B)	109	4798	3356	74
H(6C)	6	4438	1969	74
H(7B)	1701	1861	6724	70
H(7A)	1701	3139	6724	70
H(8C)	225	3187	5889	133
H(8B)	187	2390	7023	133
H(8A)	232	1923	5673	133
H(9A)	3644	1864	4048	67
H(9B)	3644	3136	4048	67
H(10C)	3751	3028	6278	130
H(10A)	4647	2683	5547	130
H(10B)	3982	1789	6090	130
H(4)	-94(1)	2500	2222(3)	42(3)



Empirical formula	$C_{32}H_{46}N_6Ni_2O_4$
Formula weight	696.17
Temperature/K	173(2)
Crystal system	monoclinic
Space group	$P2_1/c$
$a/\text{\AA}$	11.8858(11)
$b/\text{\AA}$	20.3741(18)
$c/\text{\AA}$	13.8508(13)
$\alpha/^\circ$	90
$\beta/^\circ$	100.6100(10)
$\gamma/^\circ$	90
Volume/ \AA^3	3296.8(5)
Z	4
$\rho_{\text{calc}}/\text{mg}/\text{mm}^3$	1.403
m/mm^{-1}	1.187
F(000)	1472.0
Crystal size/ mm^3	$0.669 \times 0.538 \times 0.338$
2Θ range for data collection	3.486 to 62.066°
Index ranges	$-17 \leq h \leq 17$, $-29 \leq k \leq 28$, $-20 \leq l \leq 20$
Reflections collected	32648
Independent reflections	10493[R(int) = 0.0431]
Data/restraints/parameters	10493/4/421
Goodness-of-fit on F^2	1.034
Final R indexes [$I \geq 2\sigma(I)$]	$R_1 = 0.0508$, $wR_2 = 0.1386$
Final R indexes [all data]	$R_1 = 0.0728$, $wR_2 = 0.1517$
Largest diff. peak/hole / $e \text{\AA}^{-3}$	1.12/-0.63

Table 2 Fractional Atomic Coordinates ($\times 10^4$) and Equivalent Isotropic Displacement Parameters ($\text{\AA}^2 \times 10^3$) for . U_{eq} is defined as 1/3 of the trace of the orthogonalised U_{ij} tensor.

Atom	<i>x</i>	<i>y</i>	<i>z</i>	$U(\text{eq})$
Ni1	2783.4(2)	3156.39(13)	1777.69(19)	21.90(9)
Ni2	890.8(2)	6565.13(13)	3675.9(2)	23.85(9)
O2	889.4(13)	4493.6(9)	1325.0(13)	33.0(4)
O1	3262.9(16)	3632.4(9)	-628.0(13)	35.3(4)
N5	-492.4(15)	6029.1(10)	3262.7(14)	27.4(4)
N1	4346.1(15)	2778.6(9)	2137.1(14)	27.3(4)
N2	2883.7(17)	3428.7(9)	3155.8(14)	28.3(4)
N3	2148.2(15)	4213.0(9)	293.1(13)	24.9(4)
O3	3842.8(16)	6603.2(11)	4686.6(15)	45.6(5)
N4	1325.5(17)	6375.2(11)	2400.9(14)	30.0(4)
N6	2454.5(16)	6283.1(11)	5583.7(14)	31.5(4)
O4	772.6(17)	6221.5(12)	6208.3(14)	49.0(5)
C11	2533.7(17)	4857.9(11)	161.0(15)	23.7(4)
C24	1984(2)	7125.5(12)	4470.1(19)	39.1(6)
C8	1308.2(18)	3356.0(11)	986.6(17)	27.0(4)
C7	2075(2)	3087.1(11)	397.0(17)	27.4(5)
C27	3037.3(18)	5738.7(12)	6092.2(16)	28.4(5)
C10	2584.5(19)	3632.2(11)	-55.7(16)	26.6(4)
C16	1767.4(18)	5329.1(12)	-292.9(16)	28.0(5)
C12	3672.7(17)	5029.1(12)	501.1(16)	26.7(4)
C14	3267(2)	6135.4(12)	-50.6(18)	33.0(5)
C25	2879(2)	6677.5(13)	4881.4(18)	33.9(5)
C28	3606(2)	5292.2(13)	5609.6(17)	33.2(5)
C9	1362.8(17)	4068.1(11)	921.3(16)	25.7(4)
C13	4036.4(19)	5668.0(13)	395.8(17)	31.2(5)
C5	4303(2)	2052.0(12)	2091(2)	42.0(6)
C31	3615(2)	5145.8(13)	7598.7(18)	34.2(5)
C32	3034(2)	5669.4(13)	7088.7(17)	32.3(5)
C29	4198(2)	4771.7(14)	6130.7(19)	36.9(6)
C15	2132(2)	5964.3(12)	-394.8(17)	32.5(5)
C30	4209(2)	4705.8(13)	7123.3(19)	37.7(6)
C23	1000(2)	6992.4(13)	4926.6(19)	37.5(6)
C4	4791(2)	2984.1(14)	3166.9(18)	35.0(5)
C26	1317(2)	6477.0(13)	5655.6(18)	34.4(5)
C6	5115(2)	3013.4(14)	1482(2)	35.5(5)
C3	3813(2)	3020.1(13)	3726.3(18)	34.4(5)
C1	3196(3)	4128.8(13)	3233(2)	48.7(8)
C2	1811(3)	3337.8(17)	3536(2)	45.4(7)
C19	-350(2)	5678.8(14)	2358.4(19)	39.4(6)

C17	-660(3)	5541.0(16)	4024(2)	51.0(7)
C22	2251(2)	5878.4(15)	2523(2)	42.0(6)
C20	279(2)	6111.2(15)	1759.5(18)	41.1(6)
C18	-1517(2)	6449.0(16)	3069(3)	50.5(8)
C21	1730(3)	6966.9(16)	1937(2)	50.7(8)

Table 3 Anisotropic Displacement Parameters ($\text{\AA}^2 \times 10^3$) for . The Anisotropic displacement factor exponent takes the form: $-2\pi^2[h^2a^{*2}U_{11} + \dots + 2hka \times b \times U_{12}]$

Atom	U_{11}	U_{22}	U_{33}	U_{23}	U_{13}	U_{12}
Ni1	22.68(13)	20.43(14)	22.04(14)	-1.01(10)	2.64(10)	-1.47(10)
Ni2	27.66(14)	19.49(14)	22.58(15)	-1.53(10)	-0.14(11)	-0.21(10)
O2	26.4(7)	34.5(9)	38.5(9)	-0.6(7)	6.9(7)	6.1(7)
O1	44.7(9)	34.5(9)	29.1(9)	-3.5(7)	13.4(7)	4.7(8)
N5	27.0(8)	27.2(9)	27.0(9)	-4.6(7)	1.6(7)	0.8(7)
N1	26.8(8)	24.6(9)	30.4(9)	0.6(7)	4.7(7)	-3.0(7)
N2	36.3(10)	24.3(9)	23.4(9)	0.4(7)	3.6(8)	1.1(8)
N3	25.8(8)	23.8(9)	25.3(9)	-0.4(7)	5.1(7)	1.1(7)
O3	34.2(9)	61.8(14)	38.3(10)	9.0(9)	0.5(8)	-15.8(9)
N4	33.9(9)	31.7(10)	24.2(9)	2.1(8)	4.7(8)	3.0(8)
N6	30.2(9)	36.9(11)	26.1(9)	1.6(8)	1.8(7)	-2.1(8)
O4	41.2(10)	71.6(15)	36.7(10)	1.7(10)	14.0(8)	9.2(10)
C11	25.2(9)	26.2(10)	19.4(9)	-0.3(8)	3.1(7)	2.6(8)
C24	53.5(15)	24.4(12)	33.4(13)	-4(1)	-8.1(11)	-6.3(11)
C8	21.6(9)	28.1(11)	30.0(11)	-1.2(9)	1.6(8)	-4.0(8)
C7	31.7(10)	23.4(10)	25.5(10)	-4.3(8)	0.8(8)	-3.1(8)
C27	25.7(9)	31.5(12)	26.6(10)	0.5(9)	0.7(8)	-6.8(8)
C10	29.7(10)	28.1(11)	19.5(10)	-3.7(8)	-1.7(8)	4.0(8)
C16	24.4(9)	32.1(12)	26.3(10)	-0.4(9)	1.8(8)	4.2(8)
C12	24.2(9)	30.6(11)	24.8(10)	1.3(9)	3.0(8)	4.8(8)
C14	39.3(12)	26.7(11)	36.9(12)	4.8(10)	17.2(10)	-1.6(9)
C25	35.0(11)	35.0(13)	28.1(12)	-0.3(10)	-3.6(10)	-13.4(10)
C28	32.8(11)	41.5(14)	24.9(11)	-2.4(10)	4.7(9)	-8.5(10)
C9	19.5(8)	31.8(11)	23.8(10)	0.0(8)	-1.6(7)	0.5(8)
C13	27.9(10)	35.9(13)	30.9(11)	-2.7(10)	8.4(9)	-3.1(9)
C5	35.2(12)	24.5(12)	65.5(18)	0.5(12)	7.5(12)	1.6(10)
C31	38.3(12)	37.4(13)	24.7(11)	1.4(9)	-0.3(9)	-7.5(10)
C32	32.8(11)	36.2(13)	26.9(11)	-3.2(10)	2.9(9)	-3.3(9)
C29	35.1(11)	36.1(13)	39.4(13)	-7.2(11)	7(1)	-1.9(10)
C15	36.5(11)	30.7(12)	30.9(11)	8.2(9)	8.0(9)	9.6(9)
C30	40.9(12)	31.3(12)	37.6(13)	4.7(10)	-1.6(10)	-4.2(10)
C23	46.3(14)	32.1(13)	30.8(12)	-9.6(10)	-1.2(11)	8.2(11)
C4	27.5(10)	44.1(14)	31.2(12)	3.7(10)	-0.8(9)	-3.9(10)

C26	37.0(12)	40.2(14)	24.6(11)	-10(1)	2.3(9)	2.9(10)
C6	29.4(11)	39.4(14)	39.5(13)	2.0(11)	11.2(10)	-0.8(10)
C3	35.5(11)	40.3(14)	25.4(11)	6.9(10)	0.6(9)	-0.3(10)
C1	83(2)	25.4(12)	33.9(13)	-5.1(10)	0.3(14)	-2.9(13)
C2	45.7(15)	61.3(19)	32.6(14)	4.3(13)	16.3(12)	15.4(13)
C19	38.7(12)	38.8(14)	38.7(13)	-16.9(11)	1.7(11)	-5.3(11)
C17	55.6(17)	46.3(17)	50.8(17)	2.1(14)	8.9(14)	-17.2(14)
C22	38.9(13)	46.9(16)	39.7(14)	-4.1(12)	5.7(11)	7.9(12)
C20	41.5(13)	55.4(17)	23.9(11)	-7.9(11)	-0.8(10)	-0.8(12)
C18	29.6(12)	52.4(18)	66(2)	-12.4(15)	-1.4(13)	11.2(11)
C21	66(2)	47.3(17)	40.9(16)	13.7(13)	16.8(14)	-7.1(15)

Table 4 Bond Lengths for .

Atom	Atom	Length/Å	Atom	Atom	Length/Å
Ni1	N1	1.9874(19)	N4	C21	1.487(4)
Ni1	N2	1.970(2)	N6	C27	1.424(3)
Ni1	C8	1.932(2)	N6	C25	1.424(3)
Ni1	C7	1.948(2)	N6	C26	1.430(3)
Ni2	N5	1.9690(19)	O4	C26	1.207(3)
Ni2	N4	1.967(2)	C11	C16	1.391(3)
Ni2	C24	1.917(2)	C11	C12	1.393(3)
Ni2	C23	1.922(3)	C24	C25	1.437(4)
O2	C9	1.223(3)	C24	C23	1.454(4)
O1	C10	1.230(3)	C8	C7	1.439(4)
N5	C19	1.478(3)	C8	C9	1.456(3)
N5	C17	1.490(4)	C7	C10	1.461(3)
N5	C18	1.472(3)	C27	C28	1.378(4)
N1	C5	1.482(3)	C27	C32	1.388(3)
N1	C4	1.487(3)	C16	C15	1.380(3)
N1	C6	1.481(3)	C12	C13	1.388(3)
N2	C3	1.489(3)	C14	C13	1.384(3)
N2	C1	1.473(3)	C14	C15	1.390(3)
N2	C2	1.478(4)	C28	C29	1.397(4)
N3	C11	1.414(3)	C31	C32	1.391(3)
N3	C10	1.412(3)	C31	C30	1.381(4)
N3	C9	1.419(3)	C29	C30	1.379(4)
O3	C25	1.233(3)	C23	C26	1.457(4)
N4	C22	1.481(3)	C4	C3	1.512(4)
N4	C20	1.489(3)	C19	C20	1.501(4)

Table 5 Bond Angles for .

Atom	Atom	Atom	Angle/°	Atom	Atom	Atom	Angle/°
N2	Ni1	N1	88.82(8)	C16	C11	C12	119.6(2)
C8	Ni1	N1	158.80(9)	C12	C11	N3	120.42(18)
C8	Ni1	N2	112.14(10)	C25	C24	Ni2	102.90(17)
C8	Ni1	C7	43.55(10)	C25	C24	C23	107.8(2)
C7	Ni1	N1	115.66(9)	C23	C24	Ni2	67.90(14)
C7	Ni1	N2	155.48(9)	C7	C8	Ni1	68.79(12)
N4	Ni2	N5	88.47(8)	C7	C8	C9	107.7(2)
C24	Ni2	N5	159.81(12)	C9	C8	Ni1	101.47(13)
C24	Ni2	N4	111.70(12)	C8	C7	Ni1	67.65(12)
C24	Ni2	C23	44.51(13)	C8	C7	C10	108.1(2)
C23	Ni2	N5	115.31(11)	C10	C7	Ni1	103.18(14)
C23	Ni2	N4	155.91(11)	C28	C27	N6	120.8(2)
C19	N5	Ni2	107.13(15)	C28	C27	C32	120.4(2)
C19	N5	C17	109.2(2)	C32	C27	N6	118.8(2)
C17	N5	Ni2	112.19(15)	O1	C10	N3	123.1(2)
C18	N5	Ni2	110.44(17)	O1	C10	C7	130.5(2)
C18	N5	C19	110.2(2)	N3	C10	C7	106.4(2)
C18	N5	C17	107.7(2)	C15	C16	C11	120.1(2)
C5	N1	Ni1	110.64(15)	C13	C12	C11	120.1(2)
C5	N1	C4	109.0(2)	C13	C14	C15	120.0(2)
C4	N1	Ni1	106.36(15)	O3	C25	N6	122.7(2)
C6	N1	Ni1	112.04(15)	O3	C25	C24	129.8(3)
C6	N1	C5	108.5(2)	N6	C25	C24	107.4(2)
C6	N1	C4	110.28(18)	C27	C28	C29	119.7(2)
C3	N2	Ni1	105.27(15)	O2	C9	N3	122.9(2)
C1	N2	Ni1	108.23(16)	O2	C9	C8	130.4(2)
C1	N2	C3	110.5(2)	N3	C9	C8	106.68(19)
C1	N2	C2	108.5(2)	C14	C13	C12	119.9(2)
C2	N2	Ni1	114.04(16)	C30	C31	C32	120.4(2)
C2	N2	C3	110.2(2)	C27	C32	C31	119.4(2)
C11	N3	C9	122.52(19)	C30	C29	C28	120.0(3)
C10	N3	C11	125.87(19)	C16	C15	C14	120.2(2)
C10	N3	C9	111.09(19)	C29	C30	C31	120.0(2)
C22	N4	Ni2	110.11(16)	C24	C23	Ni2	67.59(14)
C22	N4	C20	110.0(2)	C24	C23	C26	108.0(2)
C22	N4	C21	108.1(2)	C26	C23	Ni2	105.31(17)
C20	N4	Ni2	106.14(16)	N1	C4	C3	109.53(18)
C21	N4	Ni2	112.83(19)	N6	C26	C23	106.1(2)
C21	N4	C20	109.6(2)	O4	C26	N6	123.3(2)
C27	N6	C25	125.2(2)	O4	C26	C23	130.5(3)
C27	N6	C26	124.1(2)	N2	C3	C4	108.7(2)
C25	N6	C26	110.5(2)	N5	C19	C20	109.3(2)

C16 C11 N3 119.92(18) N4 C20 C19 109.20(19)

Table 6 Hydrogen Atom Coordinates ($\text{\AA}\times 10^4$) and Isotropic Displacement Parameters ($\text{\AA}^2\times 10^3$) for .

Atom	x	y	z	U(eq)
H16	1008	5216	-528	34
H12	4190	4715	799	32
H14	3510	6564	-120	40
H28	3597	5337	4940	40
H13	4796	5782	625	37
H5A	3847	1891	2545	63
H5B	5064	1879	2261	63
H5C	3968	1916	1437	63
H31	3603	5092	8263	41
H32	2647	5971	7412	39
H29	4584	4470	5808	44
H15	1616	6279	-695	39
H30	4616	4365	7473	45
H4A	5156	3410	3172	42
H4B	5357	2671	3480	42
H6A	4833	2866	824	53
H6B	5871	2842	1704	53
H6C	5140	3484	1493	53
H3A	3529	2582	3818	41
H3B	4075	3214	4368	41
H1A	3869	4199	2957	73
H1B	3345	4257	3912	73
H1C	2577	4386	2882	73
H2A	1219	3605	3165	68
H2B	1930	3464	4215	68
H2C	1586	2885	3474	68
H19A	-1095	5565	1979	47
H19B	76	5276	2528	47
H17A	6	5267	4178	77
H17B	-1317	5275	3780	77
H17C	-777	5767	4606	77
H22A	2914	6048	2953	63
H22B	2441	5780	1895	63
H22C	1997	5486	2801	63
H20A	491	5861	1225	49
H20B	-211	6470	1480	49
H18A	-1640	6643	3672	76
H18B	-2171	6189	2792	76

H18C	-1409	6789	2615	76
H21A	1155	7303	1876	76
H21B	1875	6855	1297	76
H21C	2423	7125	2337	76
H8	627(15)	3153(13)	1180(20)	33(7)
H7	2040(20)	2664(8)	58(18)	33(7)
H23	385(18)	7287(13)	5070(20)	47(9)
H24	2190(30)	7552(9)	4200(20)	54(9)

6. References

- 1 Nobelprize.org. http://www.nobelprize.org/nobel_prizes/chemistry/laureates/
(Accessed Nov 26, 2011).
- 2 a) Kochi, J.; Tamura, M. *J. Am. Chem. Soc.*, **1971**, *93*, 1483. b) Kochi, J.;
Tamura, M. *J. Am. Chem. Soc.*, **1971**, *93*, 1485. c) Kochi, J.; Tamura, M. *J.*
Organomet. Chem., **1971**, *31*, 289.
- 3 Knochel, P.; Studemann, T.; Devasagayaraj, A. *Angew. Chem., Int. Ed. Engl.*,
1995, *34*, 2723.
- 4 Percec, V.; Garg, N. K.; Rosen, B. M.; Quasdorf, K. W.; Wilson, D. A.;
Zhang, N.; Resmerita, A. *Chem. Rev.*, **2011**, *111*, 1346.
- 5 Heck, R. F. *Acc. Chem. Res.*, **1979**, *12*, 146.
- 6 Hiyama, T.; Shirakawa, E. *Top. Curr. Chem.*, **2002**, *219*, 61.
- 7 Terao, J.; Kambe, N. *Acc. Chem. Res.*, **2008**, *41*, 1545.
- 8 Negishi, E. I. *Bull. Chem. Soc. Jpn.* **2007**, *80*, 233.
- 9 Miyaura, N.; Suzuki, A. *Chem. Rev.*, **1995**, *95*, 2457.
- 10 Sonogashira, K. J. *J. Organomet. Chem.*, **2002**, *653*, 46.
- 11 Still, J. K. *Angew. Chem., Int. Ed.*, **1986**, *25*, 508.
- 12 Lau, K. S. Y.; Stille, J. K. *Acc. Chem. Res.*, **1977**, *10*, 434.
- 13 Tsou, T. T.; Kochi, J. K. *J. Am. Chem. Soc.*, **1979**, *101*, 6319.
- 14 a) Wong, K. T.; Leung, M. K.; Luh, T. Y. *Chem. Rev.*, **2000**, *100*, 3187. b)
Cardenas, D. J. *Angew. Chem., Int. Ed.*, **1999**, *38*, 3018. c) Fu, G. C.;
Netherton, M. R. *Adv. Synth. Catal.*, **2004**, *346*, 1525. d) Beller, M.; Frisch,

- A. C. *Angew. Chem., Int. Ed.*, **2005**, *44*, 674. d) Lautens, M.; Rudolph, A. *Angew. Chem., Int. Ed.* **2009**, *48*, 2656.
- 15 Hu, X. *Chem. Sci.*, **2011**, *2*, 1867.
- 16 Morokuma, K.; Koga, N.; Obara, S.; Kitaura, K. *J. Am. Chem. Soc.*, **1985**, *107*, 7109.
- 17 Wenkert, E.; Michelotti, E. L.; Swindell, C. S. *J. Am. Chem. Soc.*, **1979**, *101*, 2246.
- 18 Yu, D.; Li, B.; Shi, Z. *Acc. Chem. Res.*, **2010**, *43*, 1486.
- 19 Fu, G. C.; Zhou, J. *J. Am. Chem. Soc.*, **2003**, *125*, 14726.
- 20 Fu, G. C.; Fischer, C. *J. Am. Chem. Soc.*, **2005**, *127*, 4594.
- 21 Knochel, P.; Dussin, G.; Studemann, T.; Giovannini, R. *Angew. Chem., Int. Ed.*, **1998**, *37*, 2387.
- 22 a) Vicic, D. A.; Jones, G. D.; Anderson, T. J. *J. Am. Chem. Soc.*, **2004**, *126*, 8100. b) Vicic, D. A.; Jones, G. D.; McFarland, C.; Anderson, T. J. *Chem. Commun.*, **2005**, 4211. c) Vicic, D. A.; Jones, G. D.; Martin, J. L.; McFarland, C.; Allen, O. R.; Hall, R. E.; Haley, A. D.; Brandon, R. J.; Konovalova, T.; Desrochers, P. J.; Pulay, P. *J. Am. Chem. Soc.*, **2006**, *128*, 13175.
- 23 a) Hu, X. L.; Scopelliti, R.; Harkins, S. B.; Vechorkin, O.; Csok Z. *J. Am. Chem. Soc.*, **2008**, *130*, 8156. b) Hu, X. L.; Scopelliti, R.; Csok, Z.; Vechorkin, O. *Chem.-Eur. J.*, **2009**, *15*, 3889.
- 24 a) Hu, X. L.; Proust, V.; Vechorkin, O. *Angew. Chem., Int. Ed.* **2009**, *48*, 2937. b) Hu, X. L.; Proust, V.; Vechorkin, O. *J. Am. Chem. Soc.*, **2009**, *131*,

9756. c) Hu, X. L.; Proust, V.; Barmaz, D.; Vechorkin, O. *J. Am. Chem. Soc.*, **2009**, *131*, 12078. d) Hu, X. L.; Proust, V.; Vechorkin, O. *Angew. Chem., Int. Ed.*, **2010**, *49*, 3061. d) Hu, X. L.; Scopelliti, R.; Vechorkin, O. *Angew. Chem., Int. Ed.*, **2011**, *50*, 11777.
- 25 Kaschaube, W.; Porschke, K. R.; Wilke, G. *J. Organomet. Chem.*, **1988**, *355*, 525.
- 26 a) Collman, J. P.; Hegedus, L. S.; Norton, J. R.; Finke, R. G. *Principles and Applications of Organotransition Metal Chemistry*; University Science Books: Sausalito, Ca, 1987; pp 326 – 327. b) Ikeda, S.; Yamamoto, A.; Yamamoto, T. *J. Am. Chem. Soc.*, **1971**, *93*, 3350. c) Doyle, M. J.; Binger, P. *J. Organomet. Chem.*, **1978**, *162*, 195. d) Tatsumi, K.; Nakamura, A.; Komiya, S.; Yamamoto, A.; Yamamoto, T. *J. Am. Chem. Soc.*, **1984**, *106*, 8181. e) Komiya, S.; Akai, Y.; Tanaka, K.; Yamamoto, A.; Yamamoto, T. *Organometallics*, **1985**, *4*, 1130.
- 27 a) Huheey, J. E.; Keiter, E. A.; Keiter, R. L. *Inorganic Chemistry: Principles of Structure and Reactivity*; Prentice Hall, 1997. b) Balahura, R. J.; Lewis, N. A. *Coord. Chem. Rev.*, **1976**, *20*, 109.
- 28 Marshall, W. J.; Grushin, V. V. *Can. J. Chem.*, **2005**, *83*, 640.
- 29 a) Jenkins, A. D.; Herath, A.; Song, M.; Montgomery, J. *J. Am. Chem. Soc.*, **2011**, *133*, 14460. b) Baxter, R. D.; Montgomery, J.; *J. Am. Chem. Soc.*, **2011**, *133*, 5728. c) Li, W.; Chen, N.; Montgomery, J. *Angew. Chem. Int. Ed.*, **2010**, *47*, 8712. d) Phillips, J. H.; Montgomery, J. *Org. Lett.*, **2010**, *12*, 4556. e) Liu, P.; McCarren, P.; Cheong, P. H.-Y.; Jamison, T. F.; Houk, K. N.

J. Am. Chem. Soc., **2010**, *132*, 2050. f) McCarren, P. R.; Liu, P.; Cheong, P. H.-Y.; Jamison, T. F.; Houk, K. N. *J. Am. Chem. Soc.*, **2009**, *131*, 6654. g) Ng, S.-S.; Ho, C.-Y.; Jamison, T. F. *J. Am. Chem. Soc.*, **2006**, *128*, 11513. h) Miller, K. M.; Luanphaisarnnont, T.; Molinaro, C.; Jamison, T. F. *J. Am. Chem. Soc.*, **2004**, *126*, 4130.

30 The highly undesired formation of radical character on oxygen may be reflected from the strong bond dissociation energy of a typical O-H bond (\approx 110 kcal / mol), which is comparable to the strength of C-H bonds. This may be surprising when considering the pK_a of alcohols are approximately 16, whereas the pK_a of C-H bonds are calculated to be in the 40's.

31 Tsou, T. T.; Kochi, J. K. *J. Am. Chem. Soc.*, **1979**, *101*, 7547.

32 Schaefer, A.; Horn, H.; Ahlrichs, R. *J. Chem. Phys.*, **1992**, *97* 2571.